



Macrophage Migration Inhibitory Factor (MIF) Makes Complex Contributions to Pain-Related Hyperactivity of Nociceptors after Spinal Cord Injury

Alexis Bavencoffe,¹ Emily A. Spence,¹ Michael Y. Zhu,¹ Anibal Garza-Carbajal,¹ Kerry E. Chu,¹ Ona E. Bloom,²  Carmen W. Dessauer,¹ and  Edgar T. Walters¹

¹Department of Integrative Biology and Pharmacology, McGovern Medical School at UTHealth, Houston, Texas 77030, and ²Laboratory of Spinal Cord Injury Research, Feinstein Institutes for Medical Research, Manhasset, New York 11030

Neuropathic pain is a major, inadequately treated challenge for people with spinal cord injury (SCI). While SCI pain mechanisms are often assumed to be in the CNS, rodent studies have revealed mechanistic contributions from primary nociceptors. These neurons become chronically hyperexcitable after SCI, generating ongoing electrical activity that promotes ongoing pain. A major question is whether extrinsic chemical signals help to drive ongoing electrical activity after SCI. People living with SCI exhibit acute and chronic elevation of circulating levels of macrophage migration inhibitory factor (MIF), a cytokine implicated in preclinical pain models. Probable nociceptors isolated from male rats and exposed to an MIF concentration reported in human plasma (1 ng/ml) showed hyperactivity similar to that induced by SCI, although, surprisingly, a 10-fold higher concentration failed to increase excitability. Conditioned behavioral aversion to a chamber associated with peripheral MIF injection suggested that MIF stimulates affective pain. A MIF inhibitor, Iso-1, reversed SCI-induced hyperexcitability. Unlike chronic SCI-induced hyperexcitability, acute MIF-induced hyperexcitability was only partially abrogated by inhibiting ERK signaling. Unexpectedly, MIF concentrations that induced hyperactivity in nociceptors from naive animals, after SCI induced a long-lasting conversion from a highly excitable nonaccommodating type to a rapidly accommodating, hypoexcitable type, possibly as a homeostatic response to prolonged depolarization. Treatment with conditioned medium from cultures of DRG cells obtained after SCI was sufficient to induce MIF-dependent hyperactivity in neurons from naive rats. Thus, changes in systemic and DRG levels of MIF may help to maintain SCI-induced nociceptor hyperactivity that persistently promotes pain.

Key words: conditioned place avoidance; cytokine; depolarizing spontaneous fluctuation; DRG; hyperexcitability; hypoexcitability

Significance Statement

Chronic neuropathic pain is a major challenge for people with spinal cord injury (SCI). Pain can drastically impair quality of life, and produces substantial economic and social burdens. Available treatments, including opioids, remain inadequate. This study shows that the cytokine macrophage migration inhibitory factor (MIF) can induce pain-like behavior and plays an important role in driving persistent ongoing electrical activity in injury-detecting sensory neurons (nociceptors) in a rat SCI model. The results indicate that SCI produces an increase in MIF release within sensory ganglia. Low MIF levels potently excite nociceptors, but higher levels trigger a long-lasting hypoexcitable state. These findings suggest that therapeutic targeting of MIF in neuropathic pain states may reduce pain and sensory dysfunction by curbing nociceptor hyperactivity.

Received Apr. 22, 2021; revised May 12, 2022; accepted May 19, 2022.

Author contributions: A.B., A.G.-C., O.E.B., C.W.D., and E.T.W. designed research; A.B., E.A.S., M.Y.Z., A.G.-C., and K.E.C. performed research; A.B., E.A.S., M.Y.Z., A.G.-C., K.E.C., and E.T.W. analyzed data; A.B. wrote the first draft of the paper; A.B., E.A.S., A.G.-C., O.E.B., C.W.D., and E.T.W. edited the paper; A.B., A.G.-C., and E.T.W. wrote the paper.

This work was supported by Mission Connect Grant 017-107; TIRR Foundation to A.B.; National Institute of Neurological Diseases and Stroke Grant NS091759 to C.W.D. and E.T.W. and Grant NS111521 to E.T.W. and Michael X. Zhu; and Fondren Chair in Cellular Signaling to E.T.W. We thank Max A. Odem for consultation on the Frequency-Independent Biological Signal Identification program; and Ava Porras, Sai S. Cheruvu, and Lizeth Robinson for help with video analysis of pain-related behavior.

The authors declare no competing financial interests.

Correspondence should be addressed to Alexis Bavencoffe at Alexis.Bavencoffe@uth.tmc.edu.

<https://doi.org/10.1523/JNEUROSCI.1133-21.2022>

Copyright © 2022 the authors

Introduction

Chronic neuropathic pain affects more than half of people with spinal cord injury (SCI) (Hunt et al., 2021). It can be highly debilitating and a major clinical complaint (Störmer et al., 1997; Finnerup et al., 2001; Masri and Keller, 2012). Despite recent advances, the mechanisms of neuropathic SCI pain remain elusive and largely resistant to available treatments (Widerström-Noga, 2017; Bryce, 2018). While opioids are often prescribed, they usually become ineffective and have many adverse effects (Bryce, 2018).

Most mechanistic studies have investigated alterations in the spinal cord or brain (Hulsebosch et al., 2009; Kramer et al.,

2017), but findings in rodents indicate that mechanisms promoting chronic SCI pain are also located within neuronal somata in DRGs (Bedi et al., 2010) and in sensory terminals (Carlton et al., 2009). Following moderate spinal contusion at the thoracic level, probable nociceptors exhibit hyperexcitability and spontaneous discharge of action potentials (APs) for months after the injury (Bedi et al., 2010; Yang et al., 2014; Bavencoffe et al., 2016; Berkey et al., 2020). In the absence of classical synaptic or sensory inputs, ongoing electrical activity (OA, which includes spontaneous activity [SA]) can only be generated in a neuron by sustained depolarization of resting membrane potential (RMP), hyperpolarization of AP voltage threshold, and/or enhancement of depolarizing spontaneous fluctuations (DSFs) that bridge the gap between RMP and AP threshold, all of which contribute to OA after SCI (Odem et al., 2018). Preventing OA by knocking down Nav1.8 channels (preferentially expressed in primary nociceptors and important for the generation of their APs) was found to alleviate chronic pain after SCI (Yang et al., 2014). Thus, defining the mechanisms that promote nociceptor hyperactivity may reveal promising targets to treat chronic SCI pain.

Persistent activity of the cAMP pathway (PKA and EPAC) and activation by C-Raf of ERK are necessary for nociceptor hyperactivity after SCI (Bavencoffe et al., 2016; Berkey et al., 2020; Garza Carbajal et al., 2020). Hyperactivity after SCI may involve intrinsic alterations that include increased sensitivity to extrinsic excitatory signals (Walters, 2012, 2019), as was shown by hypersensitivity to the TRPV1 agonist, capsaicin, after SCI (Wu et al., 2013). However, little is known about the roles of extrinsic signals in promoting nociceptor hyperactivity after SCI. Extrinsic stimulation may occur in peripheral terminals and in nociceptor somata, which are exposed to CSF and blood because of their intrathecal location and lack of an effective vascular permeability barrier (Abram et al., 2006; Jimenez-Andrade et al., 2008).

Macrophage migration inhibitory factor (MIF) is an evolutionarily conserved, pleiotropic cytokine expressed in numerous cell types, including T cells, macrophages, astrocytes, and DRG neurons (Calandra and Roger, 2003; Alexander et al., 2012; Jankauskas et al., 2019). MIF can contribute to hypersensitivity in rodent peripheral pain models (Wang et al., 2010, 2011; Alexander et al., 2012). Importantly, circulating levels of MIF are increased in the plasma of people with acute and chronic SCI (Stein et al., 2013; Bank et al., 2015). MIF expression is also elevated at the spinal lesion site in a mouse SCI model (Koda et al., 2004). These observations suggest that MIF could be a significant contributor to nociceptor hyperactivity and consequent pain after SCI.

Here we test the predictions that MIF can induce an aversive behavioral state and, at physiologically relevant concentrations, induce nociceptor hyperexcitability, and that it contributes to the nociceptor hyperactivity previously linked to ongoing pain after SCI. In addition to obtaining evidence supporting these predictions, we found that a modest further increase in MIF concentration decreases nociceptor excitability, and that prior SCI greatly increases the potency of MIF in decreasing excitability, perhaps as a protective response to prolonged depolarization. MIF's hyperactive effects were partially dependent on ERK signaling. Ongoing MIF activity in cultures of DRG cells from previously injured rats produced hyperexcitability in nociceptors derived from uninjured animals, suggesting that MIF secreted within the DRG may enhance the effects of circulating MIF to promote pain.

Materials and Methods

Animals

All procedures followed the guidelines of the International Association for the Study of Pain and were approved by the McGovern Medical School Animal Care and Use Committees. Male Sprague Dawley rats (Envigo) were used for the entire study. After arrival at the McGovern Medical School animal facility, male rats (8–9 weeks old, 250–300 g, 2 per cage) were allowed to acclimate to a 12 h reversed light/dark cycle for at least 4 d before beginning experiments. Possible sex differences in the effects reported here will be the subject of a separate study. A modest sex difference in nociceptor hyperactivity after SCI was reported previously (Bedi et al., 2010).

Spinal cord injury procedure

Rat SCI surgeries (SCI group) were performed as previously described (Bedi et al., 2010; Bavencoffe et al., 2016; Berkey et al., 2020; Garza Carbajal et al., 2020). Animals were anesthetized with isoflurane (induction 4%–5%; maintenance 1%–2%, Covetrus) before a laminectomy at the vertebral T10 level was performed, followed by a dorsal contusive spinal impact (150 kilodyne, 1 s dwell time) using an Infinite Horizon Spinal Cord Impactor (Precision Systems and Instrumentation). Sham-operated rats (Sham group) received the same surgical procedure without the spinal impact. Uninjured, age-matched rats (Naive group) were also examined. Postoperative care consisted of analgesic buprenorphine hydrochloride (0.03 mg/kg in 2 ml saline; Buprenex, Reckitt Benckiser Healthcare) and the antibiotic enrofloxacin (2.5 mg/kg in 2 ml saline; Enroflox, Norbrook) injected intraperitoneally twice daily for 5 d (buprenorphine) or 10 d (enrofloxacin). Manual bladder evacuations were performed twice daily until rats recovered neurogenic bladder voiding. Animals had access to food and water *ad libitum*. The effectiveness of the SCI procedure in producing hindlimb paralysis was shown in all rats included in this study by standard scoring of motor function in both hindlimbs 1 d after surgery. All accepted SCI animals had scores of 0 or 1 (vs 21 in the Sham group) on the Basso, Beattie, and Bresnahan locomotor rating scale (Basso et al., 1995). An independent indicator of spinal damage was the occurrence of persistent hyperexcitability in nociceptors dissociated from SCI animals (Bedi et al., 2010; Odem et al., 2018).

Dissociation and culture of primary sensory neurons

An *in vitro* model was used to test dissociated DRG neurons that we have repeatedly found (in nociceptors from rats, mice, and humans) to retain injury-induced and pain-related hyperexcitability for >24 h in culture following *in vivo* conditions that produce persistent neuropathic pain (Bedi et al., 2010; Wu et al., 2013; Yang et al., 2014; Bavencoffe et al., 2016; Odem et al., 2018; Berkey et al., 2020; Laumet et al., 2020; North et al., 2022). Rats were killed using intraperitoneal injection of pentobarbital/phenytoin solution (Euthasol, 0.9 ml, Virbac AH) followed by transcardial perfusion of ice-cold PBS (Sigma-Aldrich). DRGs were harvested below vertebral T10 level down to L6. Ganglia were surgically desheathed before transfer to high-glucose DMEM culture medium (Sigma-Aldrich) containing trypsin TRL (0.3 mg/ml, Worthington Biochemical) and collagenase D (1.4 mg/ml, Roche Life Science). After 40 min incubation under constant shaking at 34°C, digested DRGs were washed by two successive centrifugations and triturated with two fire-polished glass Pasteur pipettes of decreasing diameters. Cells were plated on 8 mm glass coverslips (Warner Instruments) coated with poly-L-ornithine 0.01% (Sigma-Aldrich) in DMEM without serum or growth factors, and incubated overnight at 37°C, 5% CO₂ and 95% humidity.

For high-content microscopy (HCM), an additional step of BSA-gradient filtration was introduced after DRG cell dissociation to eliminate debris in the culture. Dissociated DRG cells were centrifuged in 15% BSA, the cell pellet resuspended in DMEM without supplements and plated on poly-L-ornithine-coated (0.01%, Sigma-Aldrich) 96-well clear-bottom plates for imaging (Corning); neuron density ~300–500 neurons per well. Cultures were incubated overnight in DMEM at 37°C, 5% CO₂ and 95% humidity in absence of growth factors or supplements.

Whole-cell patch electrophysiology

Whole-cell patch-clamp recordings were performed at room temperature (~21°C) 18–30 h after dissociation using an EPC10 USB (HEKA Elektronik) amplifier. Isolated primary sensory neurons with a soma diameter $\leq 30 \mu\text{m}$ were observed at 20 \times magnification on an IX-71 (Olympus) inverted microscope and recorded in an extracellular solution (ECS) containing the following (in mM): 140 NaCl, 3 KCl, 1.8 CaCl₂, 2 MgCl₂, 10 HEPES, and 10 glucose, which was adjusted to pH 7.4 with NaOH and 320 mOsm with sucrose. Patch pipettes were made of borosilicate glass capillaries (Sutter Instrument) with a horizontal P-97 puller (Sutter Instrument) and fire-polished with a MF-830 microforge (Narishige) to a final pipette resistance of 3–8 M Ω when filled with an intracellular solution composed of the following (in mM): 134 KCl, 1.6 MgCl₂, 13.2 NaCl, 3 EGTA, 9 HEPES, 4 Mg-ATP, and 0.3 Na-GTP, which was adjusted to pH 7.2 with KOH and 300 mOsm with sucrose. After obtaining a tight seal ($>3 \text{ G}\Omega$), the plasma membrane was ruptured to achieve whole-cell configuration under voltage clamp at -60 mV . Recordings were acquired with PatchMaster version 2x90.1 (HEKA Elektronik). The liquid junction potential was calculated to be $\sim 4.3 \text{ mV}$, and this estimate was not corrected, meaning the actual potentials were up to $\sim 4.3 \text{ mV}$ more negative than indicated in the recordings and measurements presented herein. Identification of nonaccommodating (NA) and rapidly accommodating (RA) neurons was done by stimulating primary neurons with a 2 s step protocol of injected currents (increment 5–20 pA) to 2 times rheobase (Odem et al., 2018). If repetitive discharge was observed, the neuron was classified as NA. If only a single AP was observed (at the beginning of the step), the neuron was classified as RA. Rheobase and AP voltage threshold were determined during this 2 s step protocol. OA at rest (equivalent to SA if no extrinsic stimulation was applied) was defined as any discharge occurring during the 60 s current-clamp recording ($I = 0$) after first switching to current-clamp mode (Bedi et al., 2010). OA at -45 mV was defined as any discharge occurring during a 30 s current-clamp recording with the neuron artificially held at -45 mV . This recording was made 1–2 min after the 2 s step protocol described above (Odem et al., 2018).

Measurement of DSFs of membrane potential

Whole-cell current-clamp recordings were analyzed using the Frequency-Independent Biological Signal Identification (FIBSI) program. FIBSI was written using the Anaconda (version 2019.7.0.0, Anaconda) distribution of Python (version 3.5.2) with dependencies on the NumPy and matplotlib.pyplot libraries (Cassidy et al., 2020). The FIBSI program incorporates the previously published algorithm used to analyze DSFs in our prior publications (Odem et al., 2018; Berkey et al., 2020; Garza Carbajal et al., 2020; Lopez et al., 2021; North et al., 2022). FIBSI uses the Ramer-Douglas-Peucker algorithm to detect DSFs, which were obtained from 30 s recordings sampled at 10 kHz with PatchMaster version 2x90.1 (HEKA Elektronik) and filtered with a 10 kHz Bessel filter. A user-defined 1 s sliding median function built into FIBSI was used to estimate RMP at each coordinate, and then FIBSI returned the coordinates, amplitudes, and durations of identified APs and DSFs and hyperpolarizing spontaneous fluctuations (each type with minimum amplitude and duration of 1.5 mV and 10 ms, respectively). Amplitudes for the suprathreshold DSFs eliciting APs were estimated conservatively as the difference of the most depolarized potential reached by the largest subthreshold DSF within the recording from the sliding median at that point. A minimal interval of 200 ms between any two APs was required for the second AP to be substituted by the maximal suprathreshold DSF amplitude in the recording period. If the interval between two APs was $<200 \text{ ms}$, then a substitution was performed only if the peak of a separate DSF or hyperpolarizing spontaneous fluctuation was detected between the APs (Odem et al., 2018).

Code accessibility

The FIBSI source code and detailed tutorial are available for free use, modification, and distribution on a GitHub repository, FIBSI Project by user rmccassidy (https://github.com/rmccassidy/FIBSI_program).

Table 1. Experimental design for behavioral tests

Condition	Drug (dose)	Vehicle	Route of injection	Test	Figure
Naive	MIF (50 ng)	Saline	Hindpaw	CPA	9A
Naive	MIF (50 ng)	Saline	Hindpaw	MC	9B, C
SCI	Iso-1 (30 μg)	Saline/DMSO	Intrathecal	CPP	9D
Naive	Iso-1 (30 μg)	Saline/DMSO	Intrathecal	CPP	9E

CPA, conditioned place avoidance; CPP, conditioned place preference; DMSO, dimethyl sulfoxide; MC, mechanical conflict; MIF, macrophage migration inhibitory factor; SCI, spinal cord injury.

Behavioral testing

Testers were always blinded to the treatments. In most cases, the personnel doing the testing were different from those giving injections. No tested animals were excluded from analysis. A table summarizing the experimental design for all behavioral testing is provided in Table 1.

Operant mechanical conflict (MC) test. The 3-chambered Mechanical-Conflict Avoidance System (Coy Laboratory Products) was used for operant assessment of aversion to noxious mechanical stimulation of the paws (Harte et al., 2016; Pahng et al., 2017; Odem et al., 2019). End-chamber A contained a mildly aversive bright white light, the floor of connecting chamber B had a dense array of sharp probes that could be elevated from 0–5 mm, and end-chamber C was dark. On day 1, rats were acclimated to the dark testing room (illuminated by red light) for 1 h before being placed into end-chamber A. Fifteen seconds later, the white light was turned on, and then after 35 s the door between chambers A and B was lifted (when the rat faced the door). The rat was video-recorded for 5 min as it explored all three chambers. This procedure was performed 3 times on day 1 with the probes retracted (0 mm). After each test, the MC device was sprayed and wiped with Rescue disinfectant cleaner (Covetrus). On day 2, the test procedure was repeated once with the probes at 0 mm. Naive rats were then injected with 40 μl of either MIF (50 ng) or vehicle (0.9% NaCl solution) into an anterior footpad on each hindpaw under isoflurane anesthesia. After 1 h, each rat was placed into the MC device and the test repeated with a 4 mm probe height. The 4 mm test was then given again, 60 min later. For SCI rats, injured animals were injected intrathecally after the first 4 mm probe test with either Iso-1 (30 μg) or vehicle (0.9% NaCl solution with 10% DMSO) between the L4 and L5 vertebrae under isoflurane anesthesia. After 30 min, each SCI rat was tested again with the 4 mm probe height. The minimum weight of the rats included in this study was 320 g, which was large enough to minimize chances for paws going between the probes. All trials were captured in 1080p at 120 fps with a Sony FDR-AX43 UHD 4K Handycam camcorder and scored by a blinded observer. The first crossing latency was defined as the time from lifting the door until all four paws were placed in chamber C. Each subsequent crossing was counted when two or more paws and the head of the rat entered the opposite chamber.

Conditioned place avoidance (CPA) test. Each day of testing, rats in the Naive group were acclimated to the behavior room for 1 h. On day 1, the rats were placed in a 3-compartment conditioned place preference (CPP) test device (Med Associates, MED-CPP-3013), containing white, gray, and black chambers. Light levels were set for 50% intensity in the white chamber, 90% in the gray chamber, and 40% in the black chamber. The test was designed so that differences among the chambers in color and illumination would add a competing motivation when rats decided which chamber to occupy. For rats, the brighter white chamber should be innately aversive compared with the darker black chamber, so a rat choosing to spend more time in the white chamber after an experience in the black chamber (in this case, a preceding injection of MIF) would indicate that the experience was sufficiently aversive to override the rat's innate preference, providing additional evidence for a strong aversive (presumably painful) state induced by the MIF injection. Rats were first given unrestricted access to all compartments for 15 min, and their movements recorded with an automated photodetection system. On the morning of day 2, each rat was anesthetized with isoflurane and injected subcutaneously with 40 μl of vehicle (0.9% NaCl sterile solution) into right and left hindpaw anterior footpads. After injection, the rats acclimated to the testing room. Each rat was then placed into their nonpreferred chamber (based on relative times spent in the white and black chambers on day 1) with the gate closed so the rat was confined to that

chamber. Only the black and white chambers were used for conditioning because none of the rats preferred the gray chamber. Four hours later, each rat was injected in the previously injected footpads with MIF (50 ng in 40 μ l 0.9% NaCl sterile solution). After acclimation, the rats were placed in their preferred chamber, which was now marked with a scent from Kiwi Lipsmackers chapstick on a piece of tape (Griggs et al., 2015). Two variants of this experiment were run on Naive rats, differing in the interval between injection and placement in the paired chamber, and in the time spent in the paired chamber. In one, the interval was 30 min and the duration was 30 min. In the second variant, the interval was 1 h and the duration was 2 h. These temporal parameters were based on the long latency between intraplantar injection of MIF and mechanical hypersensitivity reported in mice (Alexander et al., 2012). On day 3, rats were given unrestricted access to all three chambers for 15 min, with the chamber previously paired with MIF injection again marked with the same scent. Between each test, the chambers were cleaned thoroughly with 70% ethanol. The room lights were off during all tests, and the experimenter left the room after each rat was placed in the test device.

CPP test. A single-trial conditioning procedure was modified from those used previously to assess spontaneous pain in rats (King et al., 2009; Yang et al., 2014; Wu et al., 2017). CPP testing was performed on both Naive and SCI (1–2 months postinjury) rats. Procedures were the same as used for CPA with the following differences. On the morning of day 2, rats were injected intrathecally between the L4 and L5 vertebrae with 30 μ l vehicle (0.9% NaCl sterile solution with 10% DMSO). After injection, rats acclimated to the testing room for 30 min. Each rat was then placed into its preferred chamber (based on relative times spent in each chamber on day 1) for 30 min with the door closed. Four hours later, each rat was injected intrathecally with 30 μ l of the MIF inhibitor Iso-1 (30 μ g in 0.9% NaCl sterile solution with 10% DMSO). After 30 min acclimation, the rat was transferred into the nonpreferred chamber containing the scent mark for 30 min. On day 3, the rats were tested with access to all three chambers, including the scent-marked nonpreferred chamber.

Drug administration

Rats were anesthetized with isoflurane (4% induction and 2% maintenance) in a separate room from the behavior testing room, injected, and observed for complete recovery before being moved to the testing room. For CPA and MC tests, MIF was prepared in sterile saline solution (0.9% NaCl) at a final concentration of 50 ng in 40 μ l. Corresponding vehicle treatment consisted of 40 μ l saline injections. MIF or vehicle was injected subcutaneously into an anterior footpad on each hindpaw using an insulin syringe (28 G needle, BD U-100). For CPP, Iso-1 was prepared in DMSO at a concentration of 10 mg/ml and then diluted to a final concentration of 30 μ g in 30 μ l of saline. Vehicle consisted of 30 μ l saline with 10% DMSO. Iso-1 or vehicle was injected intrathecally using insulin syringes (28 G needle, BD U-100) in the gap between the L4 and L5 vertebrae, delivering the drugs close to the DRGs innervating the hindlimbs (L4–L6). Intrathecal injection of agents at the lumbar vertebral level has been shown previously to result in diffusion up to cervical levels (Gustafsson et al., 1985). Observation of a brisk tail flick during an injection indicated successful delivery of the drug or vehicle (Stokes et al., 2011; Njoo et al., 2014; Thomas et al., 2016).

Pharmacological agents

Recombinant human MIF was purchased from PeptoTech, dissolved with sterile water at a 50 μ g/ml stock concentration, and stored at -80° C. MIF inhibitor Iso-1 was obtained from Sigma-Aldrich, reconstituted in DMSO (Sigma-Aldrich), and stored at 42 mM in the dark at -20° C. Adenyl cyclase activator forskolin was purchased from Cayman Chemicals, prepared in DMSO at a stock concentration of 10 mM, and stored at -20° C. For electrophysiology, reagents were diluted in ECS by a minimum factor of 1/1000. UO126 was purchased from Selleck Chemicals and prepared at a 50 mM stock solution in DMSO, Recombinant Murine β -NGF (nerve growth factor) was purchased from PeptoTech and reconstituted at 20 μ g/ml stock solution. UO126 and NGF stock solutions were aliquoted and stored at -80° C.

While any drug may have off-target effects, the efficacy and specificity of Iso-1 for blocking MIF signaling are well established. Iso-1 has been shown to bind specifically within the hydrophobic pocket of MIF, blocking both the tautomerase activity and MIF's binding to its receptors (Al-Abed and VanPatten, 2011). The specificity of recognition of the MIF "pocket" structure by Iso-1 was shown by X-ray crystallography of Iso-1 bound to MIF (Lubetsky et al., 2002; Trivedi-Parmar and Jorgensen, 2018), reinforcing the widespread use of Iso-1 as the canonical MIF inhibitor. Iso-1 has been used extensively in preclinical studies as a MIF inhibitor, including rodent pain experiments (Wang et al., 2010, 2018; Alexander et al., 2012).

Cell treatments and immunofluorescence staining for HCM

Pharmacological treatments were performed at 37° C, 5% CO_2 as previously described (Isensee et al., 2014; Garza Carbajal et al., 2020). In brief, DRG neurons isolated from Naive rats were pretreated with UO126 (3 μ M) or vehicle (DMSO) for 30 min, followed by stimulation with the different compounds or vehicle for additional 30 min (MIF 1 ng/ml, NGF 30 ng/ml, or PBS). Drugs and corresponding vehicles were added to individual culture wells as $2\times$ stock solutions dissolved in 50 μ l culture supernatant (final volume per well 100 μ l, final DMSO \leq 0.1%). Treatments were terminated by fixation with 4% PFA (10 min at 22° C) followed by two PBS washes. Blocking and permeabilization of fixed cells were performed in a single step using blocking buffer (1% BSA, 0.075% Triton X-100, 1 h, room temperature). Plates were incubated with the primary antibody overnight at 4° C, followed by incubation with the secondary antibodies and DAPI for 1 h at room temperature. Both primary and secondary antibodies were prepared in blocking buffer. After a final wash, plates were sealed and imaged.

Primary antibodies used for HCM were mouse monoclonal anti phospho-p44/42 MAPK (T202/Y204) (1:1000, clone E10, Cell Signaling), anti-PGP9.5 (1:4000, Novus Biologicals). Secondary antibodies (all 1:1000) were goat anti-chicken DyLight 755, goat anti-mouse AlexaFluor-568 from Thermo Fisher Scientific as well as DAPI (1:1000).

Quantitative HCM

The protocol used was described by Garza Carbajal et al. (2020). Stained cultures in 96-well plates were scanned using a Cellomics CX5 microscope (Thermo Fisher Scientific). Images of 1104×1104 pixels were acquired with a $10\times$ objective and analyzed using the Cellomics software package (Thermo Fisher Scientific). After background correction, neurons were identified based on PGP 9.5 staining intensity. Object segmentation was performed using the geometric method. Results for each condition consist of at least three different replicate experiments performed on different days.

Experimental design and statistical analysis

The general experimental design was (1) to use MIF-treated and vehicle-treated groups of neurons or rats to test the sufficiency of MIF to produce nociceptor hyperactivity and ongoing pain, and (2) to use an MIF inhibitor to test the necessity of MIF function for nociceptor hyperactivity and ongoing pain induced by SCI. Summary data are presented as medians, means \pm SEM, or incidence expressed as percentage of neurons sampled. Datasets were tested for normality with the Shapiro–Wilk test. Normally distributed data were tested with one-way ANOVA or Brown–Forsythe and Welch ANOVA (when SDs were unequal) followed by Dunnett's multiple comparisons tests using Prism version 8.3 (GraphPad Software) or with paired Student's *t* tests. Non-normally distributed datasets were tested with the Kruskal–Wallis test followed by Dunn's multiple comparison test. Comparisons of incidence were made using Fisher's exact test with Bonferroni corrections for multiple comparisons. Detailed statistical results are reported in the figures and their legends. Statistical significance was considered as $p < 0.05$, except after Bonferroni corrections, as stated in the legends and indicated by asterisks in the figures.

Results

Physiologically relevant concentrations of MIF induce hyperactivity in probable nociceptors with a narrow dose dependence

We first asked whether primary sensory neurons isolated from Naive rats and incubated with physiologically relevant

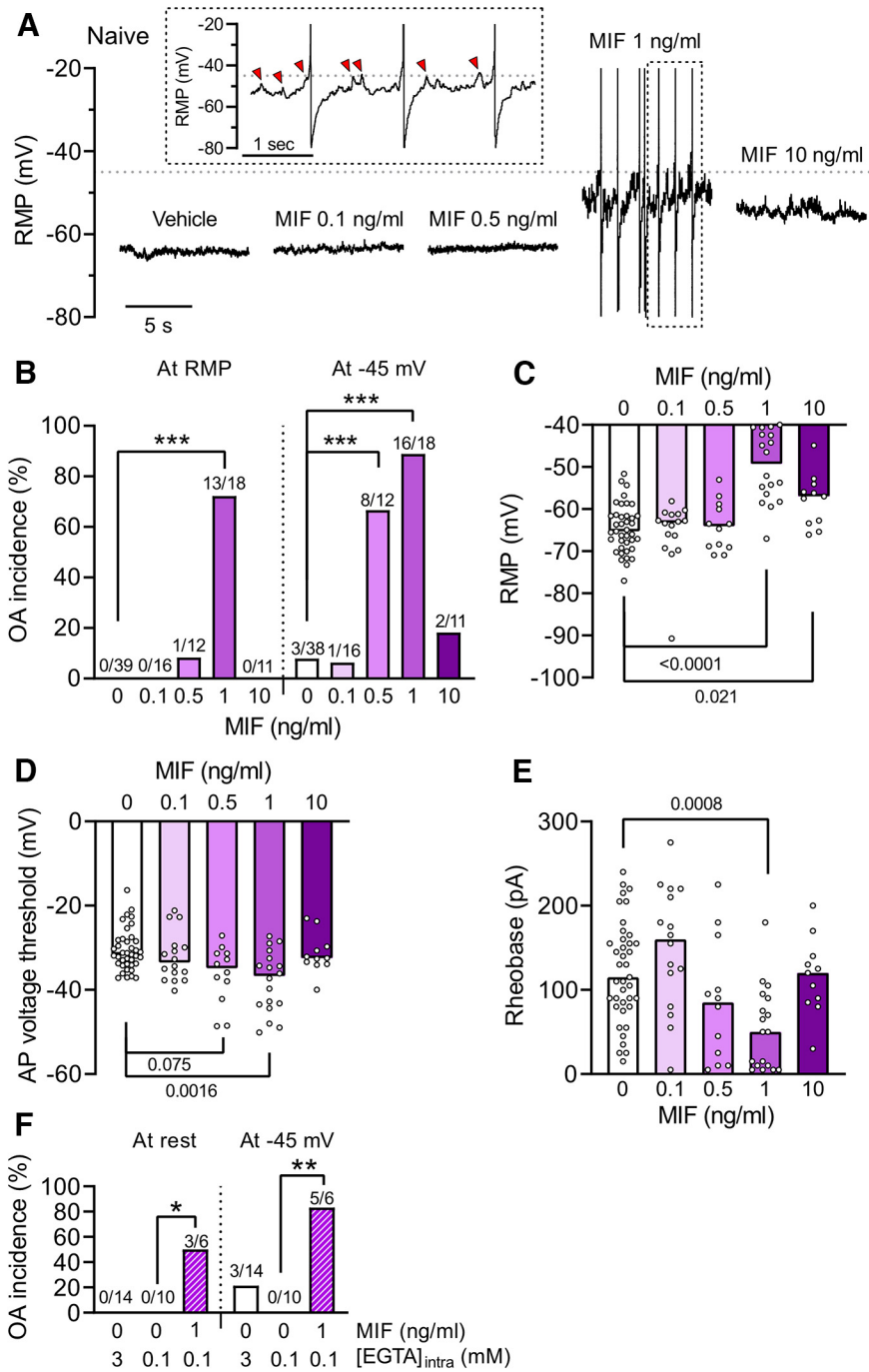


Figure 1. Brief treatment (15–60 min) of physiologically relevant concentrations of MIF increases the excitability of NA nociceptors isolated from Naive rats. **A**, Representative current-clamp recordings ($I = 0$, 10 s) from neurons during the indicated treatments. Inset, Expanded view of a 4 s segment to highlight DSFs (red arrowheads) during 1 ng/ml MIF treatment. The illustrated APs have been clipped at -20 mV to permit an enlarged view of the underlying DSFs. The actual peaks of the APs were ~ 50 mV. **B**, Effects of different doses of MIF on the incidence of neurons exhibiting OA at RMP or when artificially depolarized to -45 mV. Comparisons of OA at each concentration versus vehicle treatment (0 ng/ml) were performed with Fisher’s exact test ($*p < 0.012$ considered significant after Bonferroni correction for 4 comparisons; $**p < 0.0025$; $***p < 0.00025$). Numbers over each bar represent the number of neurons exhibiting OA/the total number sampled. **C–E**, Effects of different doses of MIF on excitability properties of NA neurons from Naive rats. **C**, RMP. **D**, AP voltage threshold. **E**, Rheobase. Each circle represents 1 neuron. Bars represent medians. Comparisons between each dose and vehicle were performed by Kruskal–Wallis tests followed by Dunn’s multiple comparison tests, with corresponding p values indicated on the figure. **F**, Lack of effects of different intracellular concentrations of EGTA (0.1 and 3 mM) on the incidence of neurons exhibiting OA at RMP or when artificially depolarized to -45 mV in the absence and presence of MIF (1 ng/ml). Comparisons of OA between basal conditions or with 0.1 mM EGTA with and without MIF were performed with Fisher’s exact tests ($*p < 0.05$; $**p < 0.01$). Numbers over each bar represent the number of neurons exhibiting OA/total number sampled.

concentrations of recombinant human MIF for 15–60 min would produce hyperactivity resembling that observed after SCI (Bedi et al., 2010). Sampling was restricted to neurons with soma diameters of 20–30 μm , $\sim 70\%$ of which we showed previously to exhibit properties of nociceptors under our culture conditions, specifically, sensitivity to capsaicin and/or binding of isolectin B4 (Bedi et al., 2010; Odem et al., 2018). Probable nociceptors *in vitro* were subclassified according to their AP accommodation properties when stimulated by a 2 s pulse of depolarizing current at twice rheobase as either RA or NA types (for examples of NA and RA neurons, see also Fig. 3A). Only NA neurons have been found to exhibit SA (defined *in vitro* as ongoing discharge at RMP in the absence of a source of extrinsic excitation applied by the experimenter) and OA (defined as any ongoing discharge; i.e., SA is a subset of OA) (Odem et al., 2018). Except where otherwise stated, all the data presented in this paper were obtained from NA neurons.

NA neurons were given 10–15 min applications of MIF at doses of 0.1–10 ng/ml (Fig. 1; Table 2) before recording, and MIF remained in the chamber for the duration of the recordings from each coverslip (up to 60 min). These concentrations overlap the range reported in human plasma acutely and chronically after SCI (medians ~ 1 ng/ml in each case, total range 0.1–8.6 ng/ml) (Stein et al., 2013; Bank et al., 2015). The 1 ng/ml dose increased the incidence of sampled neurons exhibiting OA at RMP from 0% (vehicle treatment) to 72% (Fig. 1A,B), while during artificial depolarization to -45 mV (Fig. 1B), the 0.5 and 1 ng/ml doses increased the incidence of OA from 8% (vehicle treatment) to 67% and 89%, respectively.

In terms of membrane potential, there are only three possible electrophysiological changes that can drive OA in the absence of transient depolarizing inputs, such as sensory generator potentials or synaptic potentials: depolarization of RMP, hyperpolarization of AP voltage threshold, and enhancement of DSFs (Fig. 1A, red arrowheads) that bridge the gap between RMP and AP threshold (Odem et al., 2018; North et al., 2022). The effects of MIF on RMP and on AP voltage threshold and current threshold (rheobase) are shown in Figure 1 and Table 2, and the effects on DSFs are analyzed in a subsequent section. MIF significantly depolarized RMP to median values of -49.3 mV at 1 ng/ml and -57 mV at 10 ng/ml versus -65.3 mV during vehicle treatment (Fig. 1C). MIF

Table 2. Effects of MIF on electrophysiological measures of excitability in NA neurons isolated from Naive, Sham, and SCI rats^a

	MIF (ng/ml)	0	0.1	0.5	1	10	Test
Naive	RMP (mV)	−65.3 (−77, −51.6) (39)	−63.2 (−90.7, −58.1) (16)	−64.1 (−70.9, −53) (12)	−49.3 (−67, −40) (18)***	−57 (−66.1, −44.9) (11)*	KW
	AP voltage threshold (mV)	−31.6 (−37.2, −16.3) (39)	−33.6 (−40.2, −21.2) (16)	−34.9 (−48.6, −27.1) (12)	−36.7 (−50.1, −27.3) (18)**	−32.5 (−40, −23) (11)	KW
	Rheobase (pA)	115 (15, 240) (39)	160 (5, 275) (16)	85 (5, 225) (12)	50 (5, 180) (18)***	120 (30, 200) (11)	KW
	MIF (ng/ml)	0	0.1	0.5	—	—	
Sham	RMP (mV)	−60.6 (−75.6, −50.6) (21)	−60.5 (−71.4, −40) (23)	−59.5 (−70, −44) (15)	—	—	KW
	AP voltage threshold (mV)	−30.2 (−38.8, −22.5) (21)	−27.1 (−39.4, −18.2) (23)	−30.6 (−53.4, −26.2) (14)	—	—	KW
	Rheobase (pA)	85 (10, 265) (21)	140 (0, 430) (23)	105 (5, 220) (15)	—	—	KW
	MIF (ng/ml)	0	0.01	0.1	1	—	
SCI	RMP (mV)	−48.4 (−71.4, −40) (19)	−54.2 (−78.7, −40.3) (9)	−48.8 (−68.4, −42.1) (6)	−64.3 (−68.5, −46.4) (3)	—	BF
	AP voltage threshold (mV)	−34.4 (−47.3, −29.1) (19)	−36.5 (−46.5, −20.3) (9)	−37.3 (−45.3, −32.4) (6)	−29.6 (−34.5, −23.5) (3)	—	KW
	Rheobase (pA)	35 (5, 75) (19)	65 (10, 165) (9)	20 (5, 120) (6)	85 (75, 340) (3)*	—	KW

^aValues are reported as medians (minimum, maximum) (number of cells sampled). Each dose of MIF was compared against vehicle treatment (0 ng/ml). Statistical tests: BF, Brown–Forsythe and Welch ANOVA test followed by Dunnett's T3 multiple comparison test; KW, Kruskal–Wallis test followed by Dunn's multiple comparison test.

* $p < 0.05$. ** $p < 0.01$. *** $p < 0.001$.

Table 3. MIF has little effect on electrophysiological measures of excitability in RA neurons isolated from Naive, Sham, and SCI rats^a

	MIF (ng/ml)	0	0.1	0.5	1	10	Test
Naive	RMP (mV)	−67.1 (−80.9, −55.3) (11)	−66.1 (−73.2, −59.8) (10)	−65.1 (−66.3, −62) (3)	−70.1 (−75.2, −52.6) (9)	−61 (−70, −55) (13)	BF
	AP voltage threshold (mV)	−26 (−32.6, −12.2) (11)	−29.5 (−34.4, −19.4) (10)	−30.1 (−32.4, −21.8) (3)	−24.6 (−31.5, −7) (9)	−25.3 (−34, −4.7) (13)	KW
	Rheobase (pA)	240 (40, 460) (11)	175 (100, 280) (10)	165 (100, 210) (3)	180 (135, 360) (9)	160 (40, 400) (13)	BF
	MIF (ng/ml)	0	0.1	0.5	—	—	
Sham	RMP (mV)	−65.6 (−71.2, −59) (12)	−64.2 (−73.5, −57.2) (15)	−61.1 (−62.5, −60) (4)	—	—	KW
	AP voltage threshold (mV)	−25.8 (−31.6, −14.8) (12)	−26.7 (−34.2, −16.5) (15)	−27.5 (−31.7, −25.1) (4)	—	—	KW
	Rheobase (pA)	207.5 (65, 250) (12)	215 (55, 480) (15)	172.5 (140, 260) (4)	—	—	KW
	MIF (ng/ml)	0	0.01	0.1	1	—	
SCI	RMP (mV)	−65.4 (−72.2, −60.3) (4)	−68.7 (−73.3, −64.1) (2)	−57.9 (−69.1, −46.4) (10)	−70.5 (−78.1, −52.8) (13)	—	BF
	AP voltage threshold (mV)	−33.9 (−34.7, −19.2) (4)	−31.4 (−31.4, −31.4) (2)	−24.7 (−36.5, −11.3) (10)	−29 (−37, −23.6) (13)	—	BF
	Rheobase (pA)	150 (65, 185) (4)	145 (130, 160) (2)	237.5 (100, 490) (10)	200 (100, 420) (13)	—	KW

^aValues are reported as medians (minimum, maximum) (number of cells sampled). Statistical analysis was performed by comparing each dose of MIF against vehicle (0 ng/ml). Statistical tests: BF, Brown–Forsythe and Welch ANOVA test followed by Dunnett's T3 multiple comparison test; KW, Kruskal–Wallis test followed by Dunn's multiple comparison test.

hyperpolarized the AP voltage threshold from -31.6 mV during vehicle treatment to -34.9 mV (0.5 ng/ml) and -36.7 mV (1 ng/ml) (Fig. 1D). MIF (1 ng/ml) also reduced rheobase (the minimum current needed to reach AP threshold) from 115 pA during vehicle treatment to 50 pA (Fig. 1E). No significant effects of MIF treatment were found on RA neurons (Table 3).

An unexpected finding was the unusually steep and narrow dose dependence of MIF's induction of hyperexcitability. As just described, OA, RMP, AP voltage threshold, and rheobase first showed clear changes when exogenous MIF was increased from 0.1 to either 0.5 or 1 ng/ml (Fig. 1). Surprisingly, a further increase in concentration to only 10 ng/ml reversed all of these changes (Fig. 1A–E). Compared with 1 ng/ml MIF, the 10 ng/ml dose significantly hyperpolarized RMP ($p = 0.0068$, Welch's t test), depolarized AP voltage threshold ($p = 0.0062$, Welch's t test), and increased rheobase ($p = 0.0023$, Welch's t test) (Fig. 1C–E).

We found that MIF's effects on nociceptor excitability can be rapidly reversed. Neurons from Naive rats were treated with MIF (1 ng/ml) for 15 min, which was then washed away before recording 5–60 min later. After MIF washout, no OA was recorded at RMP (data not shown, 0 of 10 neurons sampled compared with 13 of 18 exhibiting OA when MIF was not washed out, $p = 0.0003$, Fisher's exact test). MIF-induced OA recorded at -45 mV was also eliminated by MIF washout (1 of

10 with OA compared with 16 of 18 when MIF remained present, $p < 0.0001$).

Because our intracellular pipette solution contained 3 mM EGTA, we considered the possibility that some of the observed effects could have been caused by chelation producing an abnormally low intracellular Ca^{2+} concentration. However, when we used a pipette solution with only 0.1 mM EGTA, no significant differences were observed on basal electrophysiological properties (RMP, rheobase, AP voltage threshold, and OA incidence) of NA neurons from Naive rats ($n = 14$ and 10 neurons for pipette solutions containing 3 and 0.1 mM EGTA, respectively). Furthermore, we observed the same nociceptor hyperactivity triggered by MIF (1 ng/ml) with the low-EGTA pipette solution, expressed as a significant increase in OA incidence measured at rest (50% of neurons with OA) and -45 mV (83% of neurons with OA) (Fig. 1F).

Sham surgery can enhance nociceptor hyperactivity induced by MIF

The sham surgery that exposes the spinal cord for contusive SCI experiments (injuring bone, muscle, and skin) was found to produce modest but significant nociceptor hyperexcitability in the absence of SCI (Odem et al., 2018) and to enhance pain-related behavior (Odem et al., 2019) months after injury. Given these observations and the induction of hyperactivity by MIF in

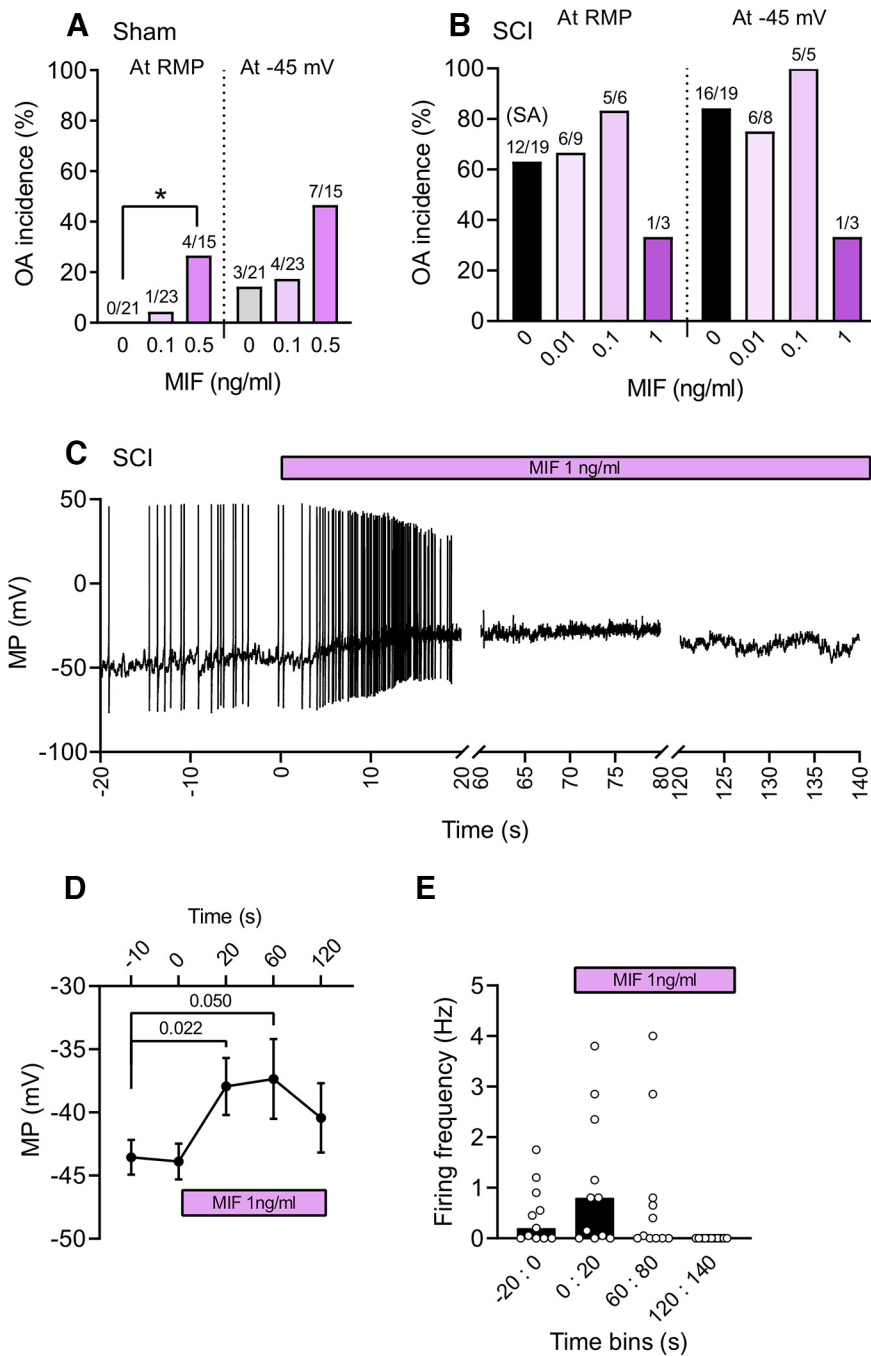


Figure 2. NA neurons isolated from injured rats exhibit complex responses to MIF. **A**, Effects of different doses of MIF (15–60 min pretreatment) on the incidence of NA neurons with OA when isolated 3–5 months after sham surgery. OA was measured at RMP and when artificially depolarized to -45 mV. Comparisons of OA at each concentration versus vehicle treatment (0 ng/ml) were performed with Fisher’s exact test ($p < 0.025$ considered significant after Bonferroni correction for 2 comparisons). **B**, Effects of MIF on the incidence of neurons with OA 1–4 months after SCI surgery ($p < 0.017$ considered significant after Bonferroni correction for 3 comparisons). **C**, Representative recording at RMP of a hyperactive NA neuron isolated from an SCI rat and exposed to MIF starting at $t = 0$. **D**, Effect of MIF exposure on mean membrane potential at different time points ($n = 11$). Comparison between control period ($t = -10$ s) with subsequent time points was performed with Friedman test followed by Dunn’s multiple comparisons test. Data are mean \pm SEM. **E**, Effect of MIF exposure on AP firing frequency measured by 20 s time bins ($n = 11$). Comparison between control period ($-20:0$ s) with subsequent time bins was performed with Friedman test followed by Dunn’s multiple comparisons test. Each circle represents 1 neuron. Bars represent medians. MP, Membrane potential.

neurons from Naive rats (Fig. 1), we predicted that nociceptors in the Sham group would display greater electrophysiological responsiveness to MIF compared with Naive controls. When tested 3–5 months after surgery at RMP, NA neurons isolated

from Sham rats and exposed to doses of MIF that did not elicit OA in neurons from Naive rats exhibited a small but significant increase in OA at 0.5 ng/ml compared with vehicle treatment (0% for vehicle treatment vs 29% for 0.5 ng/ml MIF) (Fig. 2A). When tested at -45 mV, the incidence of OA in the Sham group was 14% for vehicle treatment versus 47% for 0.5 ng/ml MIF (Fig. 2A). The promotion of hyperexcitability in NA neurons by MIF was relatively weak, as it failed to significantly alter RMP, AP voltage threshold, or rheobase (Table 2). The weakness of these effects might be explained by most of the neurons being sampled from DRGs that innervate tissues other than those injured during the sham surgery. The excitability properties of RA neurons showed no significant effects in the Sham group (Table 3).

MIF application after SCI fails to further increase nociceptor hyperactivity and promotes the transition from an NA state to an RA state

Increased sensitivity of nociceptor somata to extrinsic signals following SCI has been implied by the upregulation of growth factor receptors TrkA and TrkB in DRG neurons (Qiao and Vizzard, 2002) and the upregulation of TRPV1 in DRGs and enhanced responsiveness of nociceptors to capsaicin (Wu et al., 2013). As reported previously (Bedi et al., 2010; Bavencoffe et al., 2016; Odem et al., 2018; Berkey et al., 2020; Garza Carbajal et al., 2020), we found 1–4 months after SCI that NA neurons were significantly more likely to exhibit OA at RMP (i.e., SA), with 63% of neurons active in the SCI group (Fig. 2B) versus 0% in the Naive group (Fig. 1B). When tested at -45 mV, 84% of neurons in the SCI group had OA versus 8% in the Naive group (Figs. 1B, 2B). The increase in OA in the SCI group compared with the Naive group was accompanied by a significant depolarization of RMP ($p < 0.0001$, Brown–Forsythe and Welch ANOVA test followed by Dunnett’s T3 multiple comparison test $F_{(2,41.07)} = 20.03$, $p < 0.0001$), hyperpolarization of AP voltage threshold ($p = 0.0005$, Kruskal–Wallis test followed by Dunn’s multiple comparison test), and reduction in rheobase ($p < 0.0001$, Brown–Forsythe and Welch ANOVA test followed by Dunnett’s T3 multiple comparison test, $F_{(2,38.05)} = 15.74$, $p < 0.0001$) (Figs. 1, 2; Table 2). Unexpectedly, these chronic hyperexcitable effects of SCI were not further enhanced by MIF at any of the tested

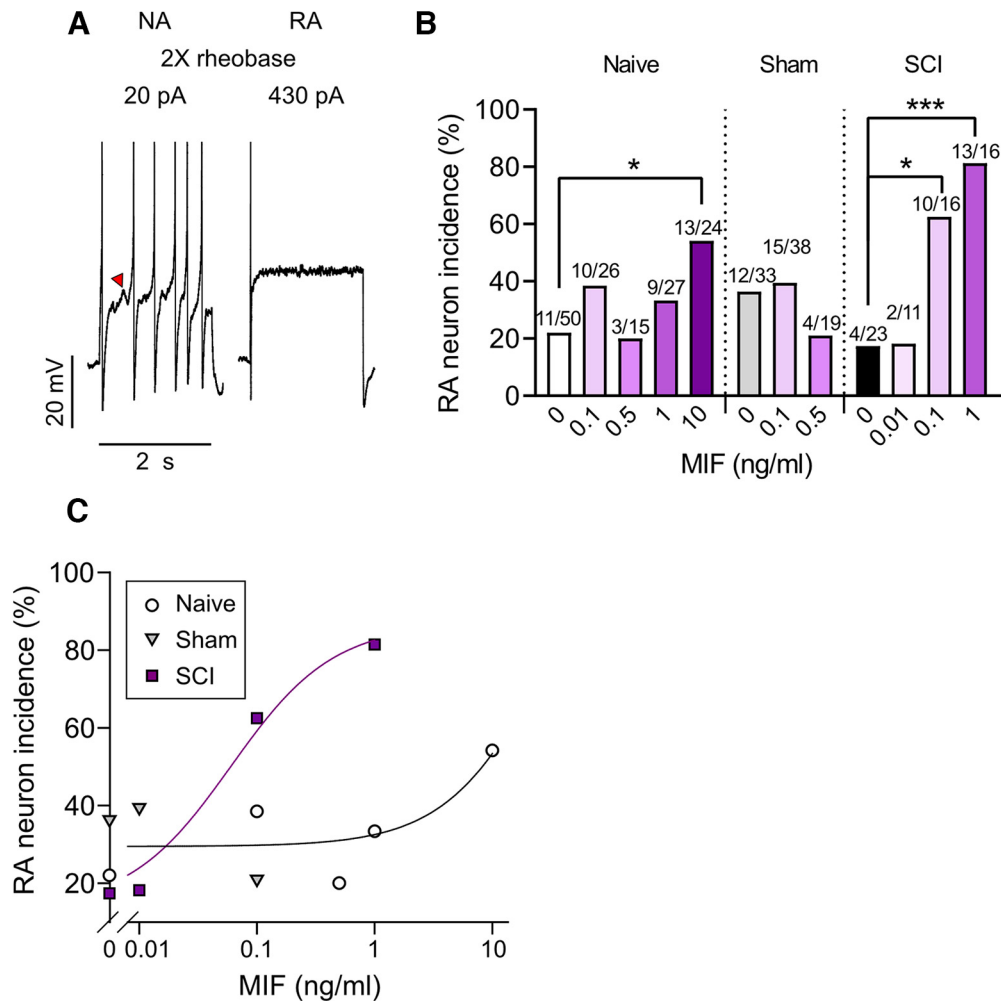


Figure 3. MIF causes a shift from NA to RA neurons after SCI. **A**, Representative traces of recordings from NA and RA neurons during a 2 s pulse of injected current at 2× rheobase. Red arrowhead indicates DSF. The illustrated APs have been clipped at 0 mV to show the DSFs. **B**, Effects of different doses of MIF on the incidence of RA neurons dissociated from Naive, Sham, and SCI rats compared with vehicle treatment. All neurons sampled were either RA or NA. Comparisons of RA incidence at each concentration versus vehicle treatment were performed with Fisher's exact test. After Bonferroni correction for multiple comparisons, the significance level was $*p < 0.012$ in the Naive group, $p < 0.025$ in the Sham group, and $p < 0.017$ in the SCI group. $***p < 0.00033$ in the SCI group. **C**, Dose–effect relationships between MIF and the incidence of RA neurons sampled from control (Naive and Sham) and SCI groups.

concentrations. Indeed, although our sample size was severely limited at the highest MIF concentration (for reasons described below), OA appeared to decrease (Fig. 2B) and rheobase increased (Table 2) when NA neurons were tested in the presence of 1 ng/ml MIF. This indicates that the neurons had become less excitable.

The failure of MIF to further increase OA (Fig. 2B) or to enhance other measures of excitability in neurons from the SCI group (Table 2) might reflect a ceiling effect or a simple shift in the dose–response relationship for MIF induced by SCI. However, combining persistent depolarization and hyperexcitability induced by SCI with strong acute depolarization of NA neurons by added MIF might induce a hypoexcitable state. To test this possibility, we perfused MIF (1 ng/ml) on NA nociceptors isolated from SCI rats. In the 20 s period following the beginning of MIF application, a pronounced depolarization of membrane potential occurred (Fig. 2C,D) often accompanied by a burst of APs (Fig. 2C,E). This discharge was followed within 60 s by inactivity that persisted during slow recovery toward the initial membrane potential (Fig. 2C–E). This pattern is consistent with a secondary response of long-lasting hypoexcitability induced during prolonged

exposure to MIF at concentrations that strongly depolarize nociceptors isolated from injured animals.

In principle, the delayed inactivity observed during prolonged depolarization (Fig. 2C,E) might function *in vivo* to protect nociceptors and/or their postsynaptic targets from excessive activation and excitotoxicity during prolonged depolarizing conditions, such as inflammation. This idea raised the possibility that the intense depolarization produced by MIF in neurons from the SCI group could trigger a transition of highly excitable NA nociceptors to much less excitable RA nociceptors during the 5–60 min period when the neurons were incubated with MIF before electrophysiological testing. The characteristic excitability differences between these nociceptor types are illustrated by the responses of NA and RA nociceptors in Figure 3A (see also Odem et al., 2018); showing the higher rheobase current, apparently higher AP threshold, and lack of repetitive discharge in the RA neuron but not the NA neuron when each was stimulated at a holding potential of -60 mV by a depolarizing current that was twice the rheobase value. A depolarization-induced shift between nociceptor types would be consistent with the lack of significant differences between NA and RA neurons in somal size, membrane capacitance, capsaicin sensitivity, and

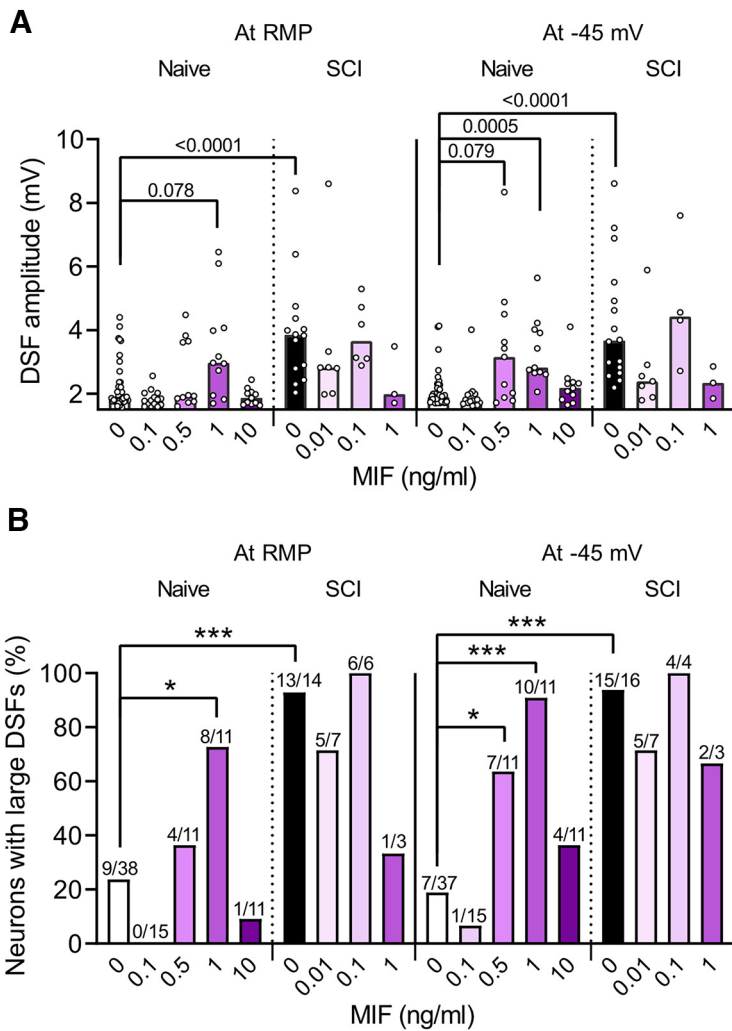


Figure 4. MIF treatment enhances DSFs in NA neurons from Naive but not SCI rats. **A**, Effects of different doses of MIF on DSF amplitudes in NA neurons isolated from Naive and SCI rats 1–4 months after surgery. Median DSF amplitudes (bars) are shown when measured at RMP and when artificially depolarized to -45 mV. Each circle represents the mean DSF amplitude measured in a 30 s recording from 1 neuron. Comparisons between each dose and vehicle (0 ng/ml) were performed by Kruskal–Wallis tests followed by Dunn’s multiple comparison tests. Comparison among Naive and SCI groups during vehicle treatment was also performed using Kruskal–Wallis tests followed by Dunn’s multiple comparison tests, with corresponding p values indicated on the figure. $p < 0.05$ was considered significant. **B**, Effects of different doses of MIF on the incidence of sampled neurons (same neurons as in **A**) with large DSFs (>5 mV) measured at RMP and when depolarized to -45 mV. Comparisons between each dose and vehicle were performed by Fisher’s exact test. After Bonferroni correction for multiple comparisons, the significance level was $*p < 0.012$ in the Naive group and $p < 0.017$ in the SCI group. $***p < 0.00025$ in the Naive group. Comparisons between Naive and SCI vehicle conditions were also performed with Fisher’s exact test, with $p < 0.025$ considered significant after Bonferroni correction. For these comparisons, the significance level was $***p < 0.0005$.

IB4 binding, and with observations that, unlike NA neurons, RA neurons never exhibit OA and are significantly less excitable than NA neurons on all tested metrics (Odem et al., 2018).

Support for a MIF-induced transition from NA to RA types came from a significant change in the relative distributions of NA and RA neurons triggered by pretreatment with lower concentrations of MIF applied to the SCI group, and also by our highest applied MIF concentration to the Naive group. Among nociceptors with a diameter ≤ 30 μ m isolated from SCI rats (all of which were classified as either NA or RA), 17% were the RA type (meaning 83% were NA) in the absence of MIF treatment (Fig. 3B,C), which was similar to the 23%–29% incidence of RA neurons after SCI we found previously in vehicle conditions for Naive and Sham groups or after SCI (Odem et al., 2018). When

exposed to 1 ng/ml of MIF, the RA incidence increased to 81% (i.e., 19% were NA) in the SCI group (Fig. 3B,C). In contrast, only 33% of sampled neurons in the Naive group were the RA type at the same MIF concentration (1 ng/ml MIF). The RA incidence increased to 54% in the Naive group treated with 10 ng/ml MIF, which was significantly elevated compared with vehicle (Fig. 3B,C), showing that, in the absence of prior injury to the animal, a sufficiently high concentration of MIF can also increase the proportion of RA neurons. The minimum doses of MIF that significantly increased RA neuron incidence was 0.1 ng/ml in the SCI group and 10 ng/ml in the Naive group (Fig. 3B,C). These results demonstrate that either a high dose of MIF by itself or the combination of a much lower dose of MIF with prior SCI can dramatically increase the incidence of RA neurons (with a corresponding decrease of NA neurons), supporting the hypothesis that the NA and RA electrophysiological signatures in our experimental conditions primarily represent different functional states rather than fixed excitability phenotypes, and that nociceptors can be induced to transition from a highly excitable NA state to a much less excitable RA state by sufficiently prolonged and intense depolarization.

MIF enhances large DSFs without apparent further amplification by SCI or sham surgery

In addition to depolarization of RMP and hyperpolarization of AP voltage threshold, the third logically possible electrophysiological change that can generate OA in isolated neurons is enhancement of DSFs (Fig. 1A, red arrowheads) that transiently exceed AP threshold (Odem et al., 2018). Automated analysis of DSFs in recordings of NA neurons from Naive rats indicated that MIF tends to increase DSF amplitudes measured at RMP at the 1 ng/ml dose, although this effect was not statistically significant (Fig. 4A). When NA neurons were artificially depolarized to -45 mV, DSF amplitudes were significantly increased by treatment with 1 ng/ml MIF in the Naive group, and a trend was seen for larger DSF amplitudes at the 0.5 ng/ml dose (Fig. 4A). While SCI increased DSF amplitudes in NA neurons measured at RMP and at -45 mV in the absence of applied MIF relative to the Naive group (0 ng/ml; Fig. 4A), no significant further increase was produced by any concentration of MIF. This might be because: (1) too few NA neurons could be found in the SCI group after treatment with 0.1 or 1 ng/ml of MIF (Fig. 2B) for sufficient statistical power, (2) a ceiling effect, (3) the few NA neurons remaining after exposure to higher MIF concentrations were a subpopulation that was unresponsive to MIF (e.g., because they did not express MIF receptors), or (4) these few NA neurons were recorded during their transition to the

RA state and had become less excitable without yet losing some of their NA properties.

The clearest effect of MIF on DSFs was on the incidence of large DSFs, defined as having amplitudes >5 mV, which is sufficient sometimes to elicit APs (Odem et al., 2018). In the Naive group, after treatment with 1 ng/ml MIF at RMP, the incidence of sampled neurons with at least one large DSF increased from 24% in vehicle-treated neurons to 73% in neurons treated with 1 ng/ml MIF (Fig. 4B). At a holding potential of -45 mV, both 0.5 and 1 ng/ml doses of MIF increased the incidence of neurons with large DSFs, from 19% to 64% and 91%, respectively (Fig. 4B), paralleling the increase in OA at -45 mV (Fig. 1B). However, no further increase in the incidence of large DSFs at RMP or -45 mV was found at any MIF dose compared with vehicle in the SCI group (Fig. 4B). Similar to the reversal in effects observed in Naive neurons when comparing the 10 ng/ml with 1 ng/ml doses on RMP (Fig. 1C), AP voltage threshold (Fig. 1D) and rheobase (Fig. 1E), we found a reversal across these doses in the relative DSF amplitudes (Fig. 4A, measured at RMP, $p = 0.0098$, Welch's t test; at -45 mV, $p = 0.0019$, Mann–Whitney t test) and in the relative incidence of neurons with large DSFs (Fig. 4B, measured at RMP, $p = 0.0075$ and -45 mV, $p = 0.024$, Fisher's exact test).

Treatment with a MIF inhibitor *in vitro* eliminates SCI-induced hyperexcitability

To assess the necessity of MIF activity *in vitro* for the occurrence of SCI-induced hyperactivity, we treated nociceptors isolated 1–4 months after surgery with a MIF inhibitor, Iso-1 (40 μ M). Iso-1 is reported to be highly specific to MIF, inhibiting MIF tautomerase activity (Lubetsky et al., 2002; Senter et al., 2002; Cheng and Al-Abed, 2006) and blocking the binding of MIF to its receptors, principally CD74, preventing activation of MIF and its downstream signaling (Al-Abed and VanPatten, 2011; Leng et al., 2011; Pantouris et al., 2015; Trivedi-Parmar and Jorgensen, 2018). Pretreatment of cultures in the SCI group with Iso-1 either overnight or beginning 1 h before testing (in both cases, Iso-1 remained present during testing) dramatically decreased the incidence of OA measured at RMP and at -45 mV (Fig. 5A). This reversal of SCI-induced hyperactivity was associated after one or both durations of Iso-1 treatment with significant alterations that would reduce hyperexcitability, including hyperpolarization of RMP (Fig. 5B), hyperpolarization of AP voltage threshold

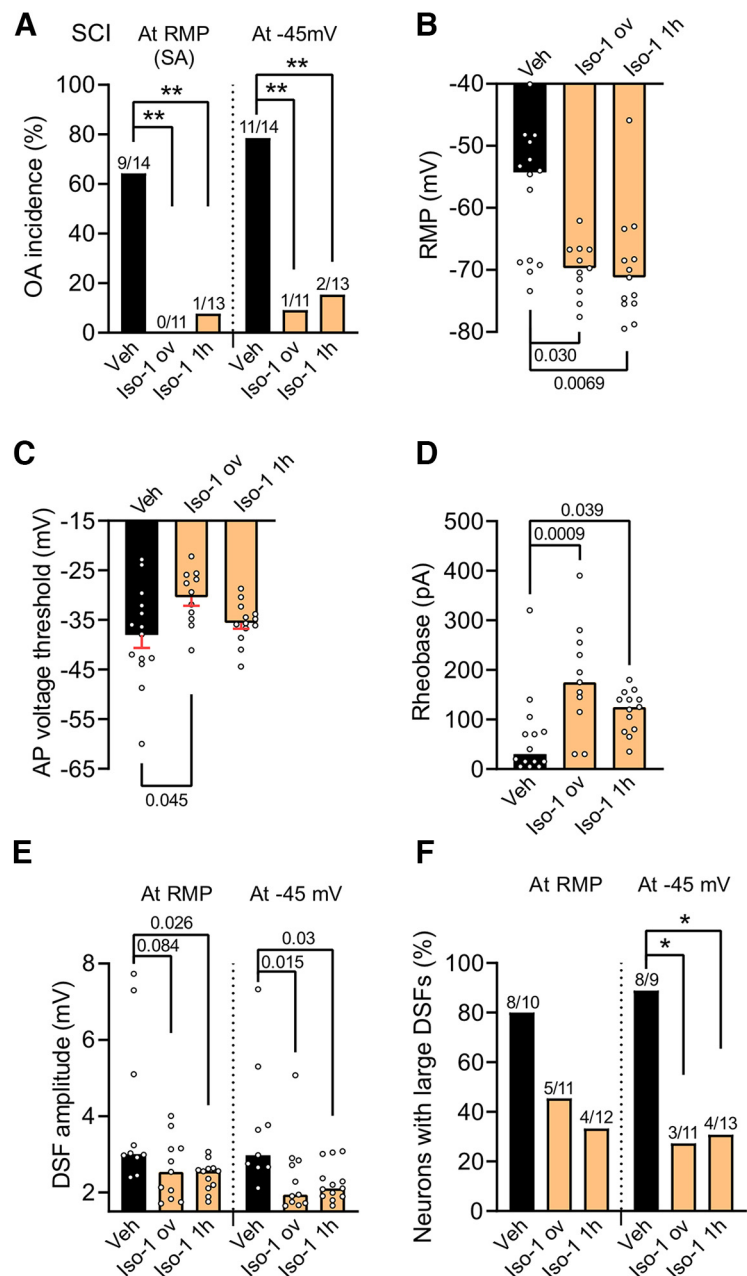


Figure 5. MIF inhibitor Iso-1 reverses hyperactivity in NA neurons from SCI rats. **A**, Effect of Iso-1 (40 μ M) treatment overnight (ov) or for 1 h before (and during) testing versus vehicle (Veh, 0.1% DMSO in ECS) on the incidence of OA recorded from NA neurons isolated from SCI rats at RMP and when depolarized to -45 mV. Comparisons of OA in each Iso-1 treatment group versus vehicle were performed with Fisher's exact test ($*p < 0.025$ considered significant after Bonferroni correction for 2 comparisons; $**p < 0.05$; $***p < 0.005$). **B**, Effects of the same treatments on median RMP. **C**, Effects on mean (\pm SEM) AP voltage threshold. **D**, Effects on median rheobase. **E**, Effects on median DSF amplitude. **F**, Effects on incidence of neurons with large (>5 mV) DSFs. Comparisons between vehicle and both Iso-1 treatments were performed by Kruskal–Wallis tests followed by Dunn's multiple comparison tests in **B** and **D**, and by Brown–Forsythe and Welch ANOVA test followed by Dunnett's T3 multiple comparison test ($F_{(2,25,81)} = 3.83$, $p = 0.035$) in **C**. **B–D**, $p < 0.05$ was considered significant. **E**, Effects of Iso-1 on median DSF amplitude measured at RMP and -45 mV. **F**, Effects of Iso-1 on the incidence of neurons with large DSFs. Comparisons between vehicle and both Iso-1 treatments were performed by Kruskal–Wallis tests followed by Dunn's multiple comparison tests in **E** and Fisher's exact test in **F**. **E**, $p < 0.05$ was considered significant. **F**, $*p < 0.025$ was considered significant after Bonferroni correction; $**p < 0.05$; $***p < 0.005$.

(Fig. 5C), and increased rheobase current (Fig. 5D). Moreover, DSF amplitudes were reduced by Iso-1 treatment when measured at RMP or -45 mV (Fig. 5E), as was the incidence of large DSFs (>5 mV) measured at -45 mV (Fig. 5F). These results show that Iso-1-sensitive signaling (probably through MIF; see Materials and

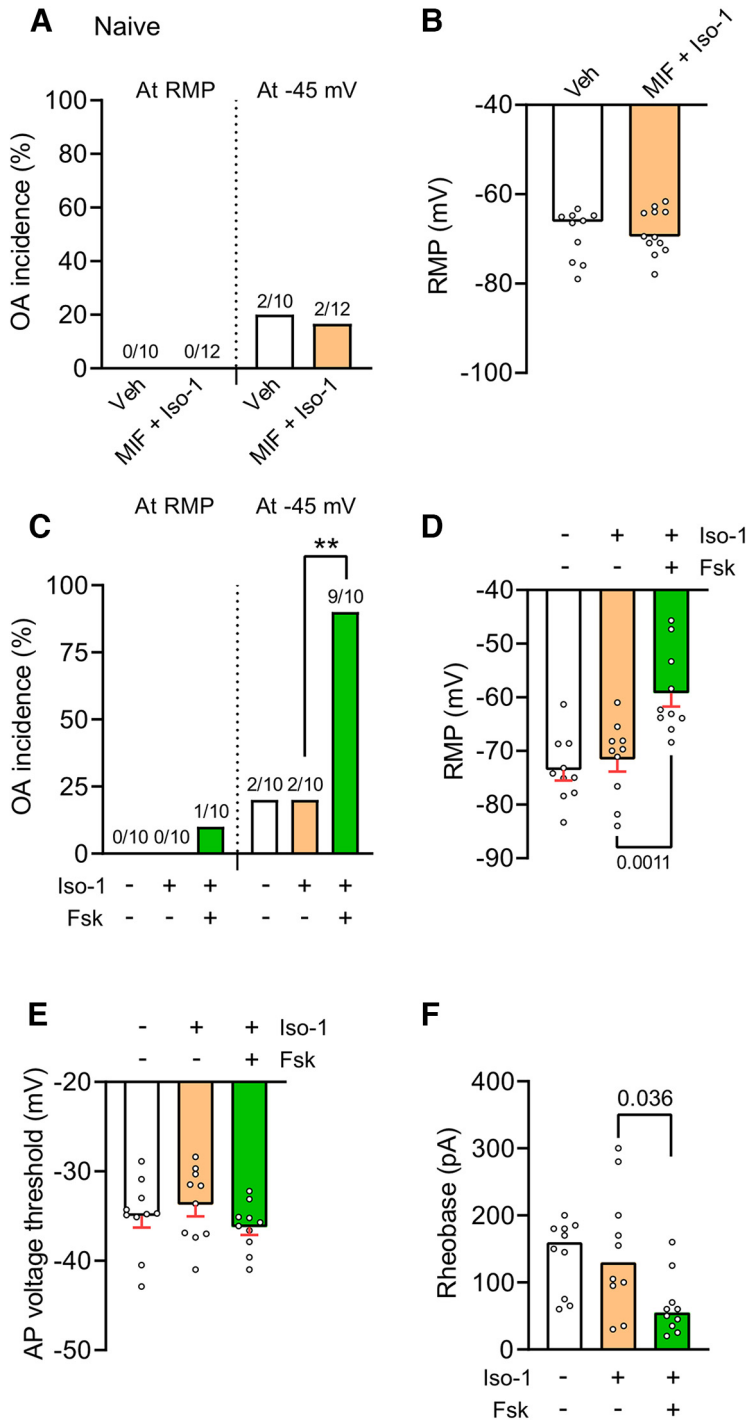


Figure 6. MIF inhibitor Iso-1 does not alter basal excitability or acute cAMP-induced hyperexcitability in NA neurons dissociated from Naive rats. **A**, Lack of effect from cocubating NA neurons with MIF (1 ng/ml, 15 min) and inhibitor Iso-1 (40 μ M, 1 h) compared with vehicle (0.1% DMSO in ECS) with on OA incidence at RMP and when depolarized to -45 mV (Fisher's exact test). **B**, Lack of effect on median RMP (Mann–Whitney *U* test). **C**, Failure of Iso-1 (40 μ M, 1 h) coapplication to prevent increased OA incidence at -45 mV by adenylyl cyclase activator forskolin (1 μ M, 15 min) (Fisher's exact test, $^{**}p < 0.005$ after Bonferroni correction). **D**, Failure of Iso-1 to prevent depolarization of mean (\pm SEM) RMP by forskolin (one-way ANOVA and Dunnett's test, $F_{(2,27)} = 0.19$, $p = 0.82$). **E**, Lack of apparent effect of Iso-1 on mean (\pm SEM) AP voltage threshold with or without forskolin (Brown–Forsythe and Welch ANOVA test and Dunnett's test, $F_{(2,24,34)} = 1.15$, $p = 0.33$). **F**, Failure of Iso-1 to prevent reduction of median rheobase by forskolin (Kruskal–Wallis test and Dunn's test). **B**, **D–F**, $p < 0.05$ was considered significant. Fsk, Forskolin; Veh, vehicle.

Methods) in the culture dish is required for the expression of nociceptor hyperactivity induced by prior SCI *in vivo*.

MIF inhibition does not alter basal excitability or acute cAMP-induced hyperexcitability in nociceptors isolated from Naive animals

An important question is how specific the strong suppression of SCI-induced hyperexcitability by MIF antagonist Iso-1 is to the hyperexcitability found after SCI. Arguing against a general neuronal effect of Iso-1 independent of SCI-induced hyperexcitability were three findings. First, while OA and hyperexcitability in neurons from the SCI group were abrogated by coapplication of Iso-1 (Fig. 5), no effects on OA incidence or RMP were found after coapplication of Iso-1 (40 μ M, 1 h) with MIF (1 ng/ml) on nociceptors from the Naive group (Fig. 6A,B), suggesting that the inhibitory effects may be specific to the increase in excitability induced by SCI. Second, pretreatment of neurons from the Naive group with Iso-1 in the absence of OA (Fig. 6C), RMP (Fig. 6D), AP voltage threshold (Fig. 6E), or rheobase (Fig. 6F). Third, as part of the experiments in Figure 6C–F, we combined Iso-1 with the adenylyl cyclase activator, forskolin (1 μ M, 15 min). As we published previously, the cAMP pathway and its downstream effectors (PKA, EPAC) are important contributors to the maintenance of nociceptor hyperactivity induced 1–8 months earlier by SCI (Bavencoffe et al., 2016; Berkey et al., 2020; Garza Carbajal et al., 2020) or acutely by serotonin (Lopez et al., 2021). Interestingly, Iso-1 failed to prevent forskolin from dramatically increasing OA measured at -45 mV (Fig. 6C) and depolarizing RMP acutely (Fig. 6D) in neurons from Naive rats. While no significant effect of Iso-1 was found on AP voltage threshold after forskolin treatment (Fig. 6E), Iso-1 did not prevent the reduction in rheobase current by forskolin (Fig. 6E). These findings indicate that Iso-1 has selective effects on nociceptors, inhibiting chronic hyperexcitability after SCI but not affecting basal excitability under Naive conditions or acute hyperexcitability induced by the stimulation of cAMP signaling by forskolin.

Conditioned medium from cultures of DRG cells isolated from SCI rats triggers MIF-dependent nociceptor hyperactivity

The inhibitory effects of Iso-1 on SCI-induced hyperactivity in dissociated nociceptors (Fig. 5) indicated that MIF function *in vitro* is necessary for promoting this hyperactivity. We next looked for evidence that MIF released into the medium from cells dissociated from SCI rats can induce hyperactivity in nociceptors dissociated from Naive rats. Our cultures include various cell types reported to express (and in some cases, release) MIF, including DRG neurons, satellite glial cells, fibroblasts, and macrophages (Abe et al., 2000; Vera and Meyer-

Siegler, 2003; Alexander et al., 2012; Lee et al., 2016), and previous studies have detected MIF expression in DRG neurons from uninjured rodents (Vera and Meyer-Siegler, 2003; Alexander et al., 2012). We first exposed nociceptors isolated from Naive rats to culture medium conditioned by overnight (~18 h) incubation of DRG cells isolated from either Naive or SCI rats (Fig. 7A). After 1 h treatment with conditioned medium, we transferred each coverslip of neurons to ECS and recorded from several sampled neurons over a period of 30–60 min. A significant increase in OA measured at -45 mV but not at RMP occurred following exposure to the SCI conditioned medium (Fig. 7B). Exposure to the Naive conditioned medium had no significant effect on OA at RMP or at -45 mV (Fig. 7B). The SCI conditioned medium produced a trend to depolarize RMP (Fig. 7C), but it had no significant effect on AP voltage threshold (Fig. 7D) or rheobase (Fig. 7E). Incubation with SCI conditioned medium increased DSF amplitudes recorded at -45 mV (Fig. 7F) and caused a large increase in the incidence of neurons with large DSFs recorded at -45 mV (Fig. 7G). Addition of Iso-1 to conditioned medium after removal of the medium from dishes containing cells from SCI animals and before transfer to dishes containing cells from Naive animals prevented the increase in OA at -45 mV (Fig. 7B), weakened the trend for depolarized RMP (Fig. 7C), and eliminated both the increase in DSF amplitude (Fig. 7F) and the increased incidence of neurons with large DSFs recorded at -45 mV (Fig. 7G). These results indicate that after SCI, an Iso-1-sensitive factor (probably MIF), is continuously released by unknown populations of dissociated DRG cells, reaching levels in the medium sufficient to induce hyperactivity lasting at least 30–60 min after washout in nociceptors isolated from rats that had not experienced SCI.

Excitation of probable nociceptors by MIF partially depends on the extracellular signal-regulated kinase (ERK) pathway

MIF stimulation of DRG neurons has been reported to involve Iso-1-sensitive binding to CD74 receptors and transactivation of the ERK pathway (Alexander et al., 2012). We recently showed that activation of the ERK pathway downstream of C-Raf is required to maintain the depolarization of RMP (into the range of ~ -55 to -50 mV) and hyperactivity in nociceptors induced by SCI (Garza Carbajal et al., 2020). Thus, we tested a possible role of the ERK pathway in the excitation of probable nociceptors by

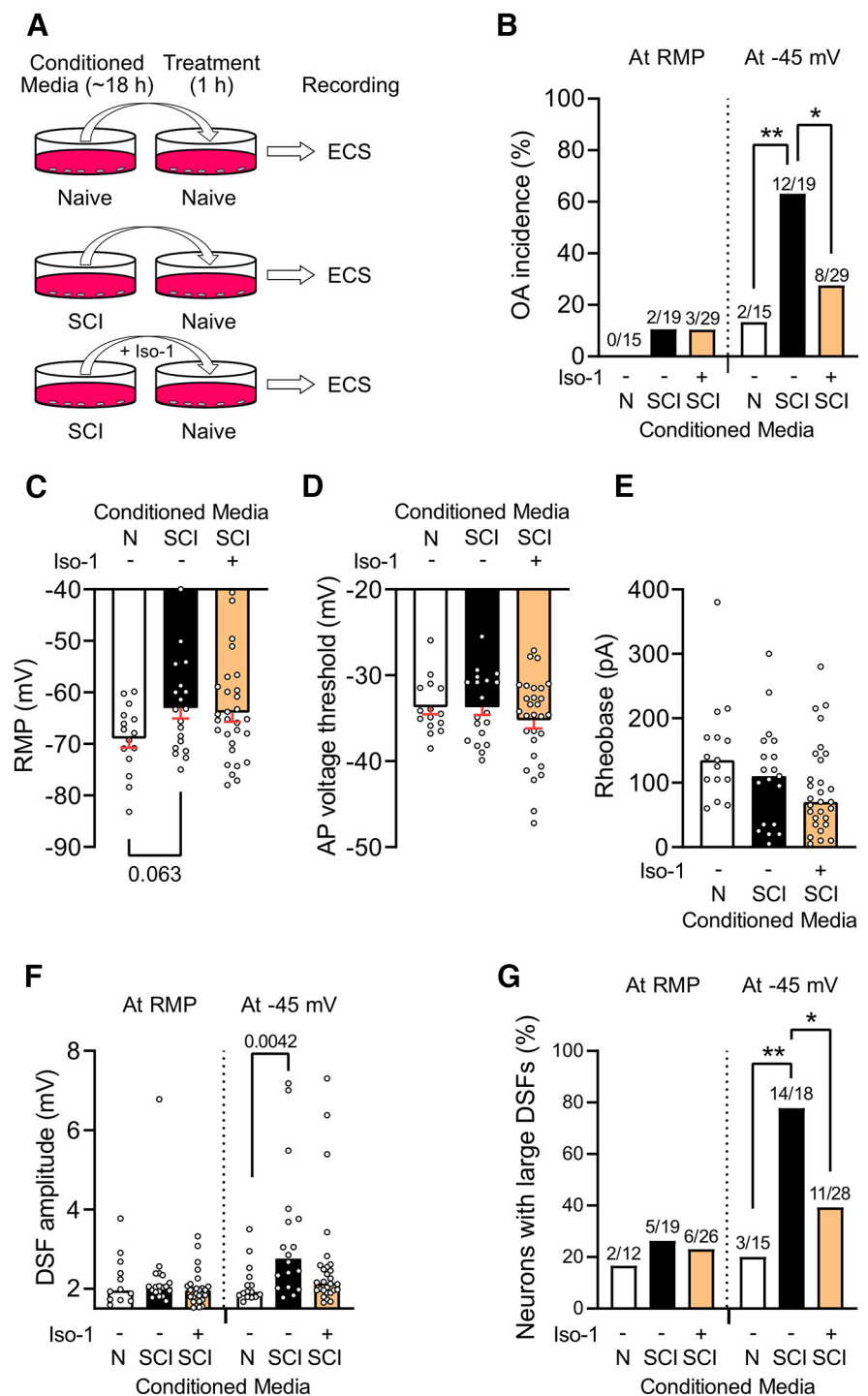


Figure 7. NA neurons dissociated from Naive rats exhibit MIF-dependent hyperactivity after exposure to conditioned medium bathing DRG cells dissociated from SCI rats. **A**, Experimental design. **B–G**, MIF-dependent effects of SCI conditioned media (SCI) versus either Naive conditioned media (N) or SCI conditioned medium plus Iso-1 (40 μ M) after 1 h on nociceptors isolated from Naive rats. **B**, Increased incidence of neurons with OA at -45 mV but not at RMP, which was prevented by Iso-1 (Fisher's exact test, $*p < 0.025$, $**p < 0.005$ after Bonferroni correction). **C**, Lack of strong effect on mean RMP (Brown–Forsythe and Welch ANOVA test followed by Dunnett's T3 multiple comparison test, $F_{(2,56.49)} = 2.5$, $p = 0.091$). **D**, Lack of effect on mean AP voltage threshold (one-way ANOVA followed by Dunnett's multiple comparison test, $F_{(2,60)} = 0.97$, $p = 0.38$). **E**, Lack of effect on median rheobase (Kruskal–Wallis test followed by Dunn's multiple comparison test). **F**, Increased median DSF amplitude measured at -45 mV but not RMP, which was prevented by Iso-1 (Kruskal–Wallis test followed by Dunn's multiple comparison test). **C–F**, $p < 0.05$ was considered significant. **G**, Increased incidence of neurons with large DSFs, which was prevented by Iso-1 (Fisher's exact test, $*p < 0.025$, $**p < 0.005$ after Bonferroni correction).

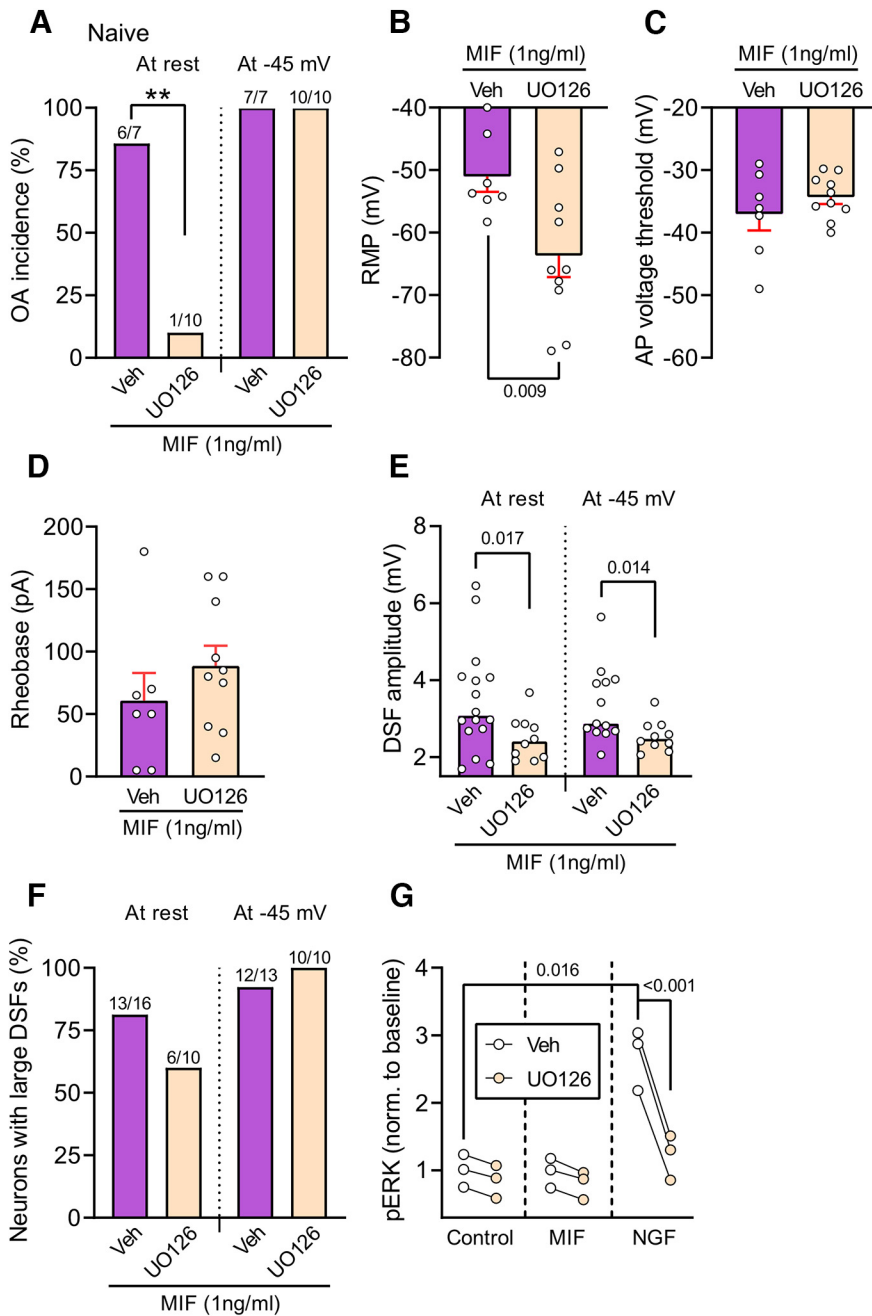


Figure 8. Partial effects of MEK/ERK inhibition on the hyperexcitable effects of MIF on NA neurons isolated from Naive rats. **A**, Effect of UO126 ($3 \mu\text{M}$) 30 min treatment versus vehicle (Veh, 0.03% DMSO in ECS) on the incidence of OA at RMP and when depolarized to -45 mV during treatment with MIF (1 ng/ml) in NA neurons from Naive rats. Neurons were treated first with vehicle or UO126 for 15 min and then cocultured with MIF for 15 min. Comparisons of OA in each treatment group versus vehicle were performed with Fisher’s exact test ($*p < 0.05$; $**p < 0.01$). **B–D**, Effects of the same treatments on mean \pm SEM RMP (**B**), AP voltage threshold (**C**), and rheobase (**D**). Comparisons were performed by Welch’s t test. **E**, Effects on median DSF amplitude. **F**, Effects on incidence of neurons with large ($>5 \text{ mV}$) DSFs. Numbers over each bar represent the number of neurons exhibiting large DSFs/total number sampled. Comparisons of DSF amplitudes between both conditions were performed by Welch’s t test, while comparisons of incidence of neurons with large DSFs were done by Fisher’s exact test. **G**, Effect of UO126 ($3 \mu\text{M}$) treatment versus vehicle (Veh, 0.03% DMSO in PBS) on pERK levels measured by HCM in control (PBS), MIF (1 ng/ml , 30 min), and NGF (30 ng/ml , 30 min) conditions. UO126 or vehicle was given 30 min beforehand. Comparisons of UO126 effects in each condition were performed by two-way ANOVA with Sidak’s multiple comparisons test ($F_{(2,12)} = 25.26$, $p = 0.0005$). Comparisons of pERK levels in vehicle conditions were done by repeated-measures one-way ANOVA with Geisser–Greenhouse correction followed by Dunnett’s multiple comparisons test ($F_{(1,1013,2,026)} = 98.39$, $p = 0.0096$).

MIF shown in Figure 1. Neurons isolated from Naive rats were pretreated with an inhibitor (UO126, $3 \mu\text{M}$) of the upstream activator of ERK, MEK (mitogen-activated protein kinase kinase), or with its corresponding vehicle (extracellular recording solution with 0.03% DMSO) for 15 min alone and then for an additional 15 min in combination with MIF (1 ng/ml). Coincubation with UO126 prevented MIF-induced OA at RMP but not at -45 mV (Fig. 8A). This effect was probably from blocking the depolarizing effects of MIF (Fig. 8B) because UO126 treatment did not significantly impact AP voltage threshold (Fig. 8C) or rheobase (Fig. 8D). Because coapplication of the vehicle for UO126 did not alter the effects of MIF (1 ng/ml), we pooled these data with the 1 ng/ml MIF data shown in Figure 1 to increase statistical power for DSF analysis. UO126 significantly decreased DSF amplitudes at rest and at -45 mV (Fig. 8E) but did not decrease the incidence of neurons with large DSFs recorded at rest or when artificially depolarized to -45 mV (Fig. 8F).

The limited impact of UO126 treatment on the hyperexcitable effects of MIF in our conditions was somewhat surprising, given that transactivation of the ERK pathway has been reported in DRGs following MIF treatment. Therefore, we determined by HCM whether MIF treatment (1 ng/ml , 15 min) increases phospho-ERK (pERK) levels acutely in sensory neurons isolated from Naive rat DRGs (Fig. 8G). We used NGF (nerve growth factor, 30 ng/ml , 30 min treatment) as a positive control (Garza Carbajal et al., 2021). While pERK levels were significantly elevated following NGF treatment compared with the control condition, there was no increase following MIF application. As expected, NGF-induced pERK elevation was prevented by 30 min treatment with UO126 ($3 \mu\text{M}$), and trends were seen for UO126 to decrease pERK in basal and MIF-stimulated conditions. These HCM data extend our electrophysiological observations of limited effects of UO126; together, they suggest that the ERK pathway contributes partially to the hyperexcitable effects of MIF on NA neurons by promoting depolarization without affecting other electrophysiological properties.

MIF can trigger an aversive behavioral state

Our observations of MIF-induced hyperexcitability and OA in probable nociceptors (see also Alexander et al., 2012) plus

previous reports of MIF-induced reflex hypersensitivity (Wang et al., 2010, 2011; Alexander et al., 2012) suggested that experimental delivery of MIF *in vivo* might produce affective pain and that inhibition of MIF activity might reduce ongoing pain. However, complexities in MIF's known actions pose challenges to documenting behavioral consequences of its activity. First, our findings of both positive and negative effects of MIF on nociceptor excitability means that injection of exogenous MIF *in vivo* might produce either net excitatory or inhibitory effects on nociceptor activity and consequent pain-related behavior, and different effects at different times and distances from an injection site. Second, previously reported behavioral effects of MIF injection *in vivo* develop over hours (Alexander et al., 2012) and possibly days (Wang et al., 2011). Slow development of complex MIF-dependent effects that might persist in the absence of MIF activity after development makes testing the behavioral roles of MIF difficult.

Our clearest indication that MIF stimulates pain was finding learned aversion to a place associated with MIF injection (conditioned place aversion [CPA]). CPA provides strong evidence for the affective-motivational component of pain in animals (Hummel et al., 2008). On day 1, all Naive rats were exposed to a three-chamber apparatus in a pretest to determine their preferred chamber. On day 2, each rat hindpaw was injected with vehicle and the rat placed later into the non-preferred chamber as determined on day 1 (vehicle pairing). Four hours later, each rat received hindpaw injections of MIF (50 ng each) and was later transferred to its previously preferred chamber (MIF pairing). On day 3, rats received a post-test identical to the pretest. In one variant of this CPA procedure, the interval between each injection and placement in the paired chamber was 30 min and the duration in the chamber was 30 min. This variant failed to produce CPA (Fig. 9A, left). Importantly, this experiment showed that nonspecific aspects of the protocol, such as where the most recent injection occurred, did not produce place aversion. The second variant of our CPA procedure assumed a longer latency and duration of MIF effects; the interval between each injection and placement in the paired chamber was 1 h, and the duration in the chamber was 2 h. This variant produced significant CPA to the MIF-paired chamber (Fig. 9A, right), revealing that stimulation by MIF can produce an aversive state resembling pain.

We used a different test of voluntary behavior to investigate potential enhancement of evoked pain (hyperalgesia) by MIF injection. A modified version (Odem et al., 2019) of a previously described operant

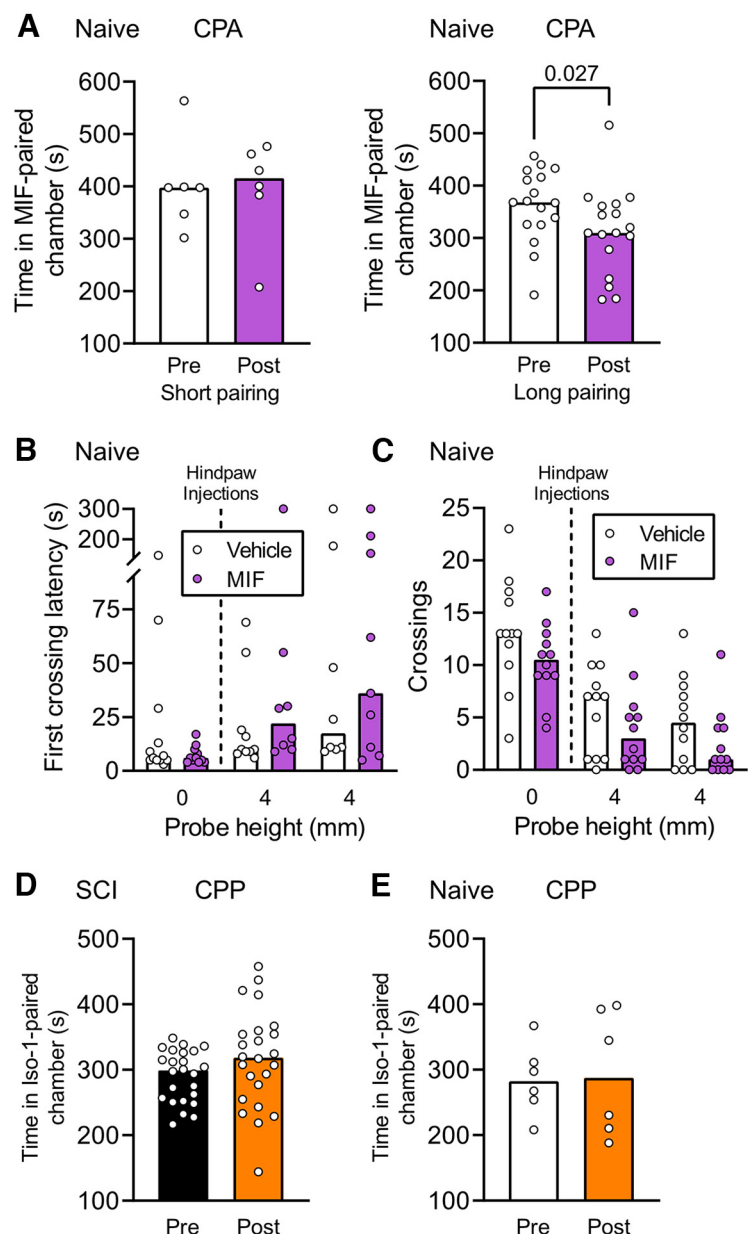


Figure 9. MIF can trigger an aversive behavioral state as indicated by CPA, but other pain-related tests did not reveal significant effects. **A**, Left, Lack of CPA to a chamber paired for a shorter period (30 min) and shorter time (30 min) after intraplantar injection of MIF (50 ng in each hindpaw). Rats received MIF in their initially preferred chamber as defined on day 1 and vehicle in their nonpreferred chamber ($n = 6$). Bars represent the median times in the initially preferred chamber. Open circles represent individual values. Differences are tested by paired t test. **A**, Right, Significant CPA to a chamber paired for a longer period (2 h) and longer time (1 h) after the MIF injections ($n = 17$). **B**, **C**, Lack of effect on the MC test from hindpaw injections of MIF (50 ng, $n = 12$) or vehicle ($n = 12$). Results from the last 3 of 6 tests are shown; only the last 2 had the sharp probes elevated to 4 mm. Injections (dashed line) were given 1 h before the first 4 mm test. **B**, Latency for the first crossing of the connecting chamber either without (0 mm) or with (4 mm) probe elevation. Both groups showed an increase in latency to cross the probes, but there were no significant treatment differences (mixed-effects two-way ANOVA with Sidak's multiple comparisons test, $F_{(1,22)} = 0.27$, $p = 0.6$). **C**, The number of crossings in 5 min. Both groups showed a decrease in crossings, but there were no significant treatment differences (two-way ANOVA with Sidak's multiple comparisons test, $F_{(1,22)} = 2.38$, $p = 0.14$). Bars represent medians. Circles represent individual animals. **D**, **E**, Results of CPP tests on SCI (**D**) and Naive rats (**E**) for a chamber paired with intrathecal injection of MIF inhibitor, Iso-1. On day 2, SCI ($n = 24$) or Naive ($n = 6$) rats received single-trial differential conditioning with intrathecal injection of Iso-1 (30 μ g) in the previously less preferred chamber, and vehicle in the other. Bars represent medians. Comparisons are by paired t test.

MC test (Harte et al., 2016; Pahng et al., 2017) gave rats a choice to cross sharp probes to explore a relatively novel environment and avoid a bright light. Mechanical hyperalgesia, as indicated by rats voluntarily choosing to spend more time under the light and to cross the probes less frequently, was revealed previously by the MC test in rats given thoracic spinal contusion or sham surgery (Odem et al., 2019). After four 5 min trials in the MC apparatus with the probes retracted (0 mm), both hindpaws of Naive rats were injected with either vehicle or MIF (50 ng). Beginning 60 min later, they were tested with the probes elevated to 4 mm, and this test was repeated after an additional 60 min. MIF injection produced no significant effects compared with vehicle on either the latency for the first crossing or the number of crossings during the 5 min tests with elevated probes (Fig. 9B,C), although a very weak trend to reduce the number of crossings at 0 and 4 mm may have been present.

We also used the MC test to see whether inhibiting MIF function would reduce evoked pain after SCI. Because the pain induced by thoracic SCI is widespread and expressed by hypersensitivity in all four limbs (Bedi et al., 2010), and because, to our knowledge, the only previous study that tested MIF inhibitors on rats' pain behavior used intrathecal injection (Wang et al., 2010), we injected either Iso-1 (30 μ g, $n = 8$) or vehicle (saline with 10% DMSO, $n = 3$) by lumbar puncture. Neither Iso-1 nor vehicle injected intrathecally after the first 4 mm probe exposure decreased the first crossing latency or increased the number of crossings during the second 4 mm probe exposure (data not shown). These results indicate that MIF injected subcutaneously into the plantar surface of a paw does not enhance affective pain evoked by stepping on sharp probes in Naive rats, and that intrathecal inhibition of MIF does not reduce chronic mechanical hyperalgesia induced by SCI.

To begin to test the hypothesis that continuing MIF activity in the DRG and/or spinal cord is required to maintain chronic ongoing pain after SCI, we used a CPP test with nearly the same schedule as our CPA tests (Fig. 9A). Previous work demonstrated a strong correlation between the incidence of SA (OA at RMP) in dissociated nociceptors and chronic reflex hypersensitivity after SCI (Bedi et al., 2010). *In vivo* interventions inhibiting SA in nociceptors (antisense knockdown of Nav1.8 channels or delivery of a KCNQ channel opener) had alleviated not only reflex hypersensitivity but also ongoing pain as indicated by a CPP test (Yang et al., 2014; Wu et al., 2017, 2020). After giving SCI rats a pretest on day 1 identical to that used in the CPA test, on day 2 vehicle was injected intrathecally 30 min before placing them into their preferred chamber for 30 min. Four hours later, the procedure was repeated with Iso-1 (30 μ g) injected intrathecally before transfer into the nonpreferred chamber. This intrathecal dose of Iso-1 was reported to reduce reflex hypersensitivity in rat models of peripheral inflammation and nerve injury (Wang et al., 2010, 2011). In the post-test on day 3, the SCI rats exhibited a very weak, statistically insignificant trend to spend more time in the chamber previously paired with Iso-1 than the chamber previously paired with vehicle injection (Fig. 9D; $p = 0.123$). The same CPP procedure on Naive rats revealed no evidence of a conditioned preference for the Iso-1-paired chamber (Fig. 9E, paired t test). Thus, while our CPA results show that MIF application can produce a pain-like aversive state, our MC and CPP tests confirm that the behavioral actions of MIF are complex, and their potential contributions to the maintenance of persistent pain after SCI require further investigation.

Discussion

This study has revealed complex roles of MIF in pain-related nociceptor activity. Importantly, conditioned avoidance of a place paired with MIF injection showed that MIF can produce an aversive, pain-like state. Physiologically relevant concentrations of MIF induced hyperactivity in dissociated nociceptors by multiple neurophysiological mechanisms. The complexity of MIF's actions was indicated by the narrow dose dependence of nociceptor hyperactivity induced by exogenous MIF, and the switch to induce hypoactivity after prior SCI. An MIF inhibitor blocked SCI-induced nociceptor hyperexcitability, and also blocked hyperexcitability induced by medium conditioned by DRG cells from SCI rats, but it did not alter basal excitability under normal conditions or forskolin-induced acute hyperexcitability.

MIF injection can produce an aversive, pain-like state

The sufficiency of MIF to induce reflex hypersensitivity was indicated previously in mice by intraplantar injection (Alexander et al., 2012) and intrathecal injection (Wang et al., 2011), which reduced paw withdrawal thresholds for several hours and 1 week, respectively. In contrast, we found only weak hints using the MC test in rats that intraplantar injection of MIF might induce mechanical hyperalgesia. Furthermore, plantar MIF injection failed to produce heat hyperalgesia or mechanical allodynia in tested rats (A.G.B., E.T.W., unpublished observations). Although this discrepancy might represent species differences, it might also reflect complicated temporal, regional, and dose dependencies of MIF actions. Importantly, we found that intraplantar MIF injection produced significant CPA, showing for the first time that MIF can induce an aversive, pain-like state. On the other hand, we did not find alleviation of SCI-induced mechanical hyperalgesia by Iso-1, nor statistically significant CPP to a chamber paired with MIF inhibitor, Iso-1, after SCI. Nevertheless, the weak trend observed for Iso-1-induced CPP encourages systematic exploration of factors (temporal, dose, route of delivery) in MIF inhibitor experiments that may reveal specific contributions of ongoing MIF activity to SCI pain that can be correlated with altered excitability of nociceptors.

MIF potently induces hyperactivity in dissociated nociceptors

While plasma levels of MIF have not been reported in rats, in humans circulating MIF levels increase from ~ 0.5 ng/ml in the absence of injury to ~ 1 ng/ml both in the first week after SCI (Bank et al., 2015) and chronically (years to decades) after SCI (Stein et al., 2013). We found that nociceptors in the Naive group showed increased OA at these same concentrations (0.5 and 1 ng/ml), accompanied by corresponding alterations in neurophysiological mechanisms promoting OA: depolarization of RMP, hyperpolarization of AP voltage threshold, and enhancement of DSFs. These same alterations occur after SCI (Odem et al., 2018; Berkey et al., 2020) and cisplatin treatment (Laumet et al., 2020) in rodents, and in human DRG neurons associated with patient-reported pain (North et al., 2022). The only previous evidence for MIF altering sensory neuron excitability (also at 1 ng/ml) was an increase in discharge frequency of OA recorded at a holding potential of ~ -30 mV in neurons isolated from Naive mice (Alexander et al., 2012).

MIF concentrations that normally produce hyperexcitability can convert NA nociceptors that are already hyperexcitable into a hypoexcitable RA state

An unusual feature of MIF's effects on the excitability of nociceptors from Naive rats was the steep and narrow dose dependence,

going from no effect to maximal effect and back to no effect over less than a 100-fold concentration range. For comparison, serotonin increases excitability without any decrease over a 1000-fold range as assessed with the same tests (Lopez et al., 2021). A possible explanation is that additional depolarization evoked by MIF concentrations >1 ng/ml *in vitro* triggers a hypoexcitable state. Our recordings from SCI neurons before and during MIF perfusion support this interpretation. Serotonin may be less likely to induce hypoexcitability because, while it decreases AP threshold and enhances DSFs, it fails to depolarize nociceptors (Lopez et al., 2021). An inverted U-shaped dose–response relationship was also described for ectopic firing of C- and A δ -fibers exposed sequentially to increasing doses of TNF α *in vivo* (Sorkin et al., 1997), supporting the possibility that nociceptors become less excitable when overstimulated by cytokines. Moreover, hypoexcitability of dissociated nociceptors after 24 h depolarization produced by KCl has been described in a preliminary report (McIlvried et al., 2018). If prolonged depolarization of nociceptors induces a hypoexcitable state, one would predict that conditions that cause hyperexcitability, such as SCI, combined with excitatory stimulation by MIF, would increase the incidence of hypoexcitable nociceptors. RA nociceptors appear identical to NA nociceptors, even in the amplitudes and durations of their APs, but they are far less excitable and fail to discharge repetitively (Odem et al., 2018). Thus, the increase in the incidence of RA neurons (and corresponding decrease in NA neurons) at the highest MIF concentration applied to the Naive group and the dramatic, long-lasting (for at least tens of minutes) shift in the hyperexcitable SCI group from NA neurons to RA neurons after treatment with lower doses of MIF are striking. These observations suggest that prolonged depolarization of sufficient amplitude and/or duration by MIF, especially when amplified by preexisting hyperexcitability induced by SCI, triggers a hypoexcitable state. This inducible state might be a dysfunctional consequence of abnormal depolarization, but it might also have protective, homeostatic functions.

MIF may be released by DRG cells to promote nociceptor hyperactivity

Nociceptor hyperactivity induced *in vitro* by concentrations of MIF found in the plasma of people with SCI (Stein et al., 2013; Bank et al., 2015) suggests that circulating MIF contributes to ongoing SCI pain driven by nociceptor OA. Unexpectedly, we found evidence that MIF may also be released by cells within the DRG. First, Iso-1 addition to DRG cultures from SCI rats inhibited nociceptor hyperexcitability. Second, conditioned medium from cultures of DRG cells from SCI rats induced a high incidence of OA and enhanced DSFs in nociceptors from Naive rats, and both effects were prevented by addition of Iso-1 to medium taken from the SCI-associated cultures. This indicates that MIF is continuously released into the medium bathing cells dissociated from SCI rats, where it helps to maintain nociceptor hyperexcitability. The potency of MIF or other factors released into the medium in response to local MIF release for driving hyperactivity is suggested by the ability of the SCI conditioned medium to promote nociceptor hyperactivity despite likely dilution of MIF compared with *in situ* conditions. Among the potential sources of MIF in our cultures are DRG neurons, satellite glial cells, fibroblasts, and macrophages, all of which may express MIF (Abe et al., 2000; Vera and Meyer-Sieglar, 2003; Alexander et al., 2012; Lee et al., 2016). Because MIF can stimulate numerous cell types (Calandra and Roger, 2003), it might exert some of its effects by triggering the release of other signals. For example,

sensory neurons exposed to conditioned media from synovio-cytes stimulated by TNF α , or satellite glial cells after cisplatin treatment, exhibited hyperexcitability potentially mediated by IL-6 (Chakrabarti et al., 2020; Leo et al., 2021). Thus, an important question concerns the extent to which MIF's effects on nociceptors represent direct excitation as opposed to indirect effects from MIF triggering the release of excitatory factors from other cell types, such as myeloid cells (Alexander et al., 2012; Cox et al., 2013).

ERK signaling is necessary for MIF-induced depolarization of nociceptors

Little is known about intracellular mechanisms for MIF's hyperexcitable effects on nociceptors. Iso-1 blocks the tautomerase activity of MIF, preventing its binding to receptors, such as CD74 and activation of pathways including ERK1/2 (Al-Abed and VanPatten, 2011; Leng et al., 2011; Pantouris et al., 2015). CD74 receptors are expressed in rodent DRGs (Mecklenburg et al., 2020; Sun et al., 2020), with increased levels after injury (Sun et al., 2020). Interestingly, ERK activity has been implicated in MIF effects on DRG (Alexander et al., 2012) and spinal neurons (Wang et al., 2010, 2011). We found that ERK inhibitor UO126 reversed MIF-induced OA at rest, depolarization of RMP, and enhancement of DSF amplitude, supporting a role for ERK signaling. However, no significant effects were observed on AP threshold, rheobase, or OA at -45 mV, indicating that ERK signaling may primarily be involved in depolarization of RMP, which then enables OA at rest (SA) and may enhance DSF amplitudes (Odem et al., 2018). This partial contribution of ERK signaling to MIF-induced hyperexcitability extends our recent finding that ERK signaling maintains SCI-induced depolarization in nociceptors (Garza Carbajal et al., 2020). An interesting possibility is that MIF-dependent depolarization helps to maintain a positive feedback loop between ERK activity and depolarization in nociceptors (Garza Carbajal et al., 2020), which contributes to persistent pain states.

In conclusion, MIF potently excites nociceptors and can stimulate a pain-like aversive state. An inhibitor of MIF attenuates nociceptor hyperexcitability induced by SCI, but not basal excitability or forskolin-induced hyperexcitability, suggesting a role of MIF released by DRGs (in addition to blood-borne MIF) for maintaining pain-related nociceptor hyperactivity after SCI. Given that neutralization of MIF reduces pathophysiology in diverse models of chronic inflammation (e.g., Stosic-Grujcic et al., 2009; Sinitski et al., 2019), inhibiting MIF may be a useful approach to treat chronic pain in SCI and related neuropathic conditions.

References

- Abe R, Shimizu T, Ohkawara A, Nishihira J (2000) Enhancement of macrophage migration inhibitory factor (MIF) expression in injured epidermis and cultured fibroblasts. *Biochim Biophys Acta* 1500:1–9.
- Abraham SE, Yi J, Fuchs A, Hogan QH (2006) Permeability of injured and intact peripheral nerves and dorsal root ganglia. *Anesthesiology* 105:146–153.
- Al-Abed Y, VanPatten S (2011) MIF as a disease target: ISO-1 as a proof-of-concept therapeutic. *Future Med Chem* 3:45–63.
- Alexander JK, Cox GM, Tian J, Zha AM, Wei P, Kigerl KA, Reddy MK, Dagia NM, Sielecki T, Zhu MX, Satoskar AR, McTigue DM, Whitacre CC, Popovich PG (2012) Macrophage migration inhibitory factor (MIF) is essential for inflammatory and neuropathic pain and enhances pain in response to stress. *Exp Neurol* 236:351–362.
- Bank M, Stein A, Sison C, Glazer A, Jassal N, McCarthy D, Shatzner M, Hahn B, Chugh R, Davies P, Bloom O (2015) Elevated circulating levels of the

- pro-inflammatory cytokine macrophage migration inhibitory factor in individuals with acute spinal cord injury. *Arch Phys Med Rehabil* 96:633–644.
- Basso DM, Beattie MS, Bresnahan JC (1995) A sensitive and reliable locomotor rating scale for open field testing in rats. *J Neurotrauma* 12:1–21.
- Bavencoffe A, Li Y, Wu Z, Yang Q, Herrera J, Kennedy EJ, Walters ET, Dessauer CW (2016) Persistent electrical activity in primary nociceptors after spinal cord injury is maintained by scaffolded adenylyl cyclase and protein kinase A and is associated with altered adenylyl cyclase regulation. *J Neurosci* 36:1660–1668.
- Bedi SS, Yang Q, Crook RJ, Du J, Wu Z, Fishman HM, Grill RJ, Carlton SM, Walters ET (2010) Chronic spontaneous activity generated in the somata of primary nociceptors is associated with pain-related behavior after spinal cord injury. *J Neurosci* 30:14870–14882.
- Berkey SC, Herrera JJ, Odem MA, Rahman S, Cheruvu SS, Cheng X, Walters ET, Dessauer CW, Bavencoffe AG (2020) EPAC1 and EPAC2 promote nociceptor hyperactivity associated with chronic pain after spinal cord injury. *Neurobiol Pain* 7:100040.
- Bryce TN (2018) Opioids should not be prescribed for chronic pain after spinal cord injury. *Spinal Cord Ser Cases* 4:66.
- Calandra T, Roger T (2003) Macrophage migration inhibitory factor: a regulator of innate immunity. *Nat Rev Immunol* 3:791–800.
- Carlton SM, Du J, Tan HY, Nesic O, Hargett GL, Bopp AC, Yamani A, Lin Q, Willis WD, Hulsebosch CE (2009) Peripheral and central sensitization in remote spinal cord regions contribute to central neuropathic pain after spinal cord injury. *Pain* 147:265–276.
- Cassidy RM, Bavencoffe AG, Lopez ER, Cheruvu SS, Walters ET, Uribe RA, Krachler AM, Odem MA (2020) Frequency-independent biological signal identification (FIBSI): a free program that simplifies intensive analysis of non-stationary time series data. *bioRxiv*. doi: 10.1101/2020.05.29.123042.
- Chakrabarti S, Hore Z, Pattison LA, Lalnunhlmi S, Bhebhe CN, Callejo G, Bulmer DC, Taams LS, Denk F, Smith ES (2020) Sensitization of knee-innervating sensory neurons by tumor necrosis factor- α -activated fibroblast-like synoviocytes: an in vitro, coculture model of inflammatory pain. *Pain* 161:2129–2141.
- Cheng KF, Al-Abed Y (2006) Critical modifications of the ISO-1 scaffold improve its potent inhibition of macrophage migration inhibitory factor (MIF) tautomerase activity. *Bioorg Med Chem Lett* 16:3376–3379.
- Cox GM, Kithcart AP, Pitt D, Guan Z, Alexander J, Williams JL, Shawler T, Dagia NM, Popovich PG, Satoskar AR, Whitacre CC (2013) Macrophage migration inhibitory factor potentiates autoimmune-mediated neuroinflammation. *J Immunol* 191:1043–1054.
- Finnerup NB, Johannesen IL, Sindrup SH, Bach FW, Jensen TS (2001) Pain and dysesthesia in patients with spinal cord injury: a postal survey. *Spinal Cord* 39:256–262.
- Garza Carbajal A, Bavencoffe A, Walters ET, Dessauer CW (2020) Depolarization-dependent C-raf signaling promotes hyperexcitability and reduces opioid sensitivity of isolated nociceptors after spinal cord injury. *J Neurosci* 40:6522–6535.
- Garza Carbajal A, Ebersberger A, Thiel A, Ferrari L, Acuna J, Brosig S, Isensee J, Moeller K, Siobal M, Rose-John S, Levine J, Schaible HG, Hucho T (2021) Oncostatin M induces hyperalgesic priming and amplifies signaling of cAMP to ERK by RapGEF2 and PKA. *J Neurochem* 157:1821–1837.
- Pantouris G, Syed MA, Fan C, Rajasekaran D, Cho TY, Rosenberg EM, Bucala R, Bhandari V, Lolis EJ (2015) An analysis of MIF structural features that control functional activation of CD74 in brief. *Chem Biol* 22:1197–1205.
- Griggs RB, Bardo MT, Taylor BK (2015) Gabapentin alleviates affective pain after traumatic nerve injury. *Neuroreport* 26:522–527.
- Gustafsson LL, Post C, Edvardsen B, Ramsay CH (1985) Distribution of morphine and meperidine after intrathecal administration in rat and mouse. *Anesthesiology* 63:483–489.
- Harte SE, Meyers JB, Donahue RR, Taylor BK, Morrow TJ (2016) Mechanical conflict system: a novel operant method for the assessment of nociceptive behavior. *PLoS One* 11:e0150164.
- Hulsebosch CE, Hains BC, Crown ED, Carlton SM (2009) Mechanisms of chronic central neuropathic pain after spinal cord injury. *Brain Res Rev* 60:202–213.
- Hummel M, Lu P, Cummons TA, Whiteside GT (2008) The persistence of a long-term negative affective state following the induction of either acute or chronic pain. *Pain* 140:436–445.
- Hunt C, Moman R, Peterson A, Wilson R, Covington S, Mustafa R, Murad MH, Hooten WM (2021) Prevalence of chronic pain after spinal cord injury: a systematic review and meta-analysis. *Reg Anesth Pain Med* 46:328–336.
- Isensee J, Diskar M, Waldherr S, Buschow R, Hasenauer J, Prinz A, Allgöwer F, Herberg FW, Hucho T (2014) Pain modulators regulate the dynamics of PKA-RII phosphorylation in subgroups of sensory neurons. *J Cell Sci* 127:216–229.
- Jankauskas SS, Wong DW, Bucala R, Djurdjaj S, Boor P (2019) Evolving complexity of MIF signaling. *Cell Signal* 57:76–88.
- Jimenez-Andrade JM, Herrera MB, Ghilardi JR, Vardanyan M, Melemedjian OK, Mantyh PW (2008) Vascularization of the dorsal root ganglia and peripheral nerve of the mouse: implications for chemical-induced peripheral sensory neuropathies. *Mol Pain* 4:10.
- King T, Vera-Portocarrero L, Gutierrez T, Vanderah TW, Dussor G, Lai J, Fields HL, Porreca F (2009) Unmasking the tonic-aversive state in neuropathic pain. *Nat Neurosci* 12:1364–1366.
- Koda M, Nishio Y, Hashimoto M, Kamada T, Koshizuka S, Yoshinaga K, Onodera S, Nishihira J, Moriya H, Yamazaki M (2004) Up-regulation of macrophage migration-inhibitory factor expression after compression-induced spinal cord injury in rats. *Acta Neuropathol* 108:31–36.
- Kramer JL, Minhas NK, Jutzeler CR, Erskine EL, Liu LJ, Ramer MS (2017) Neuropathic pain following traumatic spinal cord injury: models, measurement, and mechanisms. *J Neurosci Res* 95:1295–1306.
- Laumet G, Bavencoffe A, Edralin JD, Huo XJ, Walters ET, Dantzer R, Heijnen CJ, Kavelaars A (2020) Interleukin-10 resolves pain hypersensitivity induced by cisplatin by reversing sensory neuron hyperexcitability. *Pain* 161:2344–2352.
- Lee JP, Foote A, Fan H, Peral de Castro C, Lang T, Jones SA, Gavrilescu N, Mills KH, Leech M, Morand EF, Harris J (2016) Loss of autophagy enhances MIF/macrophage migration inhibitory factor release by macrophages. *Autophagy* 12:907–916.
- Leng L, Chen L, Fan J, Greven D, Arjona A, Du X, Austin D, Kashgarian M, Yin Z, Huang XR, Lan HY, Lolis E, Nikolic-Paterson D, Bucala R (2011) A small-molecule macrophage migration inhibitory factor antagonist protects against glomerulonephritis in lupus-prone NZB/NZW F1 and MRL/lpr mice. *J Immunol* 186:527–538.
- Leo M, Schmitt LI, Kutritz A, Kleinschnitz C, Hagenacker T (2021) Cisplatin-induced activation and functional modulation of satellite glial cells lead to cytokine-mediated modulation of sensory neuron excitability. *Exp Neurol* 341:113695.
- Lopez ER, Carbajal AG, Tian JB, Bavencoffe A, Zhu MX, Dessauer CW, Walters ET (2021) Serotonin enhances depolarizing spontaneous fluctuations, excitability, and ongoing activity in isolated rat DRG neurons via 5-HT4 receptors and cAMP-dependent mechanisms. *Neuropharmacology* 184:108408.
- Lubetsky JB, Dios A, Han J, Aljabari B, Ruzsicska B, Mitchell R, Lolis E, Al-Abed Y (2002) The tautomerase active site of macrophage migration inhibitory factor is a potential target for discovery of novel anti-inflammatory agents. *J Biol Chem* 277:24976–24982.
- Masri R, Keller A (2012) Chronic pain following spinal cord injury. In: *Advances in experimental medicine and biology*, pp 74–88. New York: Springer.
- McIlvried L, Pullen M, Gereau R (2018) Homeostatic regulation of intrinsic plasticity in mouse and human peripheral nociceptors. *J Pain* 19:S10.
- Mecklenburg J, Zou Y, Wangzhou A, Garcia D, Lai Z, Tumanov AV, Dussor G, Price TJ, Akopian AN (2020) Transcriptomic sex differences in sensory neuronal populations of mice. *Sci Rep* 10:18.
- Njoo C, Heinel C, Kuner R (2014) In vivo siRNA transfection and gene knockdown in spinal cord via rapid noninvasive lumbar intrathecal injections in mice. *J Vis Exp* 22:51229.
- North RY, Odem MA, Li Y, Tatsui CE, Cassidy RM, Dougherty PM, Walters ET (2022) Electrophysiological alterations driving pain-associated spontaneous activity in human sensory neuron somata parallel alterations described in spontaneously active rodent nociceptors. *J Pain*. Advanced online publication. Retrieved Mar 12, 2022. doi: 10.1016/j.jpain.2022.02.009.
- Odem MA, Bavencoffe AG, Cassidy RM, Lopez ER, Tian J, Dessauer CW, Walters ET (2018) Isolated nociceptors reveal multiple specializations for generating irregular ongoing activity associated with ongoing pain. *Pain* 159:2347–2362.

- Odem MA, Lacagnina MJ, Katzen SL, Li J, Spence EA, Grace PM, Walters ET (2019) Sham surgeries for central and peripheral neural injuries persistently enhance pain-avoidance behavior as revealed by an operant conflict test. *Pain* 160:2440–2455.
- Pahng AR, Paulsen RI, McGinn MA, Edwards KN, Edwards S (2017) Neurobiological correlates of pain avoidance-like behavior in morphine-dependent and non-dependent rats. *Neuroscience* 366:1–14.
- Qiao L, Vizzard MA (2002) Up-regulation of tyrosine kinase (Trka, Trkb) receptor expression and phosphorylation in lumbosacral dorsal root ganglia after chronic spinal cord (T8-T10) injury. *J Comp Neurol* 449:217–230.
- Senter PD, Al-Abed Y, Metz CN, Benigni F, Mitchell RA, Chesney J, Han J, Gartner CG, Nelson SD, Todaro GJ, Bucala R (2002) Inhibition of macrophage migration inhibitory factor (MIF) tautomerase and biological activities by acetaminophen metabolites. *Proc Natl Acad Sci USA* 99:144–149.
- Sinitski D, Kontos C, Krammer C, Asare Y, Kapurniotu A, Bernhagen J (2019) Macrophage migration inhibitory factor (MIF)-based therapeutic concepts in atherosclerosis and inflammation. *Thromb Haemostasis* 119:553–566.
- Sorkin LS, Xiao WH, Wagner R, Myers RR (1997) Tumour necrosis factor- α induces ectopic activity in nociceptive primary afferent fibres. *Neuroscience* 81:255–262.
- Stein A, Panjwani A, Sison C, Rosen L, Chugh R, Metz C, Bank M, Bloom O (2013) Pilot study: elevated circulating levels of the proinflammatory cytokine macrophage migration inhibitory factor in patients with chronic spinal cord injury. *Arch Phys Med Rehabil* 94:1498–1507.
- Stokes JA, Corr M, Yaksh TL (2011) Transient tactile allodynia following intrathecal puncture in mouse: contributions of Toll-like receptor signaling. *Neurosci Lett* 504:215–218.
- Störmer S, Gerner HJ, Grüniger W, Metzmacher K, Föllinger S, Wienke C, Aldinger W, Walker N, Zimmermann M, Paeslack V (1997) Chronic pain/dysaesthesiae in spinal cord injury patients: results of a multicentre study. *Spinal Cord* 35:446–455.
- Stosic-Grujicic S, Stojanovic I, Nicoletti F (2009) MIF in autoimmunity and novel therapeutic approaches. *Autoimmun Rev* 8:244–249.
- Sun W, Kou D, Yu Z, Yang S, Jiang C, Xiong D, Xiao L, Deng Q, Xie H, Hao Y (2020) A transcriptomic analysis of neuropathic pain in rat dorsal root ganglia following peripheral nerve injury. *Neuromolecular Med* 22:250–263.
- Thomas A, Miller A, Roughan J, Malik A, Haylor K, Sandersen C, Flecknell P, Leach M (2016) Efficacy of intrathecal morphine in a model of surgical pain in rats. *PLoS One* 11:e0163909.
- Trivedi-Parmar V, Jorgensen WL (2018) Advances and insights for small molecule inhibition of macrophage migration inhibitory factor. *J Med Chem* 61:8104–8119.
- Vera PL, Meyer-Siegler KL (2003) Anatomical location of macrophage migration inhibitory factor in urogenital tissues, peripheral ganglia and lumbosacral spinal cord of the rat. *BMC Neurosci* 4:17.
- Walters ET (2012) Nociceptors as chronic drivers of pain and hyperreflexia after spinal cord injury: an adaptive-maladaptive hyperfunctional state hypothesis. *Front Physiol* 3:309.
- Walters ET (2019) Adaptive mechanisms driving maladaptive pain: how chronic ongoing activity in primary nociceptors can enhance evolutionary fitness after severe injury. *Philos Trans R Soc Lond B Biol Sci* 374:20190277.
- Wang FZ, Shen XF, Guo XR, Peng YZ, Liu YS, Xu SQ, Yang J (2010) Spinal macrophage migration inhibitory factor contributes to the pathogenesis of inflammatory hyperalgesia in rats. *Pain* 148:275–283.
- Wang FZ, Xu SQ, Shen XF, Guo XR, Peng YZ, Yang J (2011) Spinal macrophage migration inhibitory factor is a major contributor to rodent neuropathic pain-like hypersensitivity. *Anesthesiology* 114:643–659.
- Wang X, Ma S, Wu H, Shen X, Xu S, Guo X, Bolick ML, Wu S, Wang F (2018) Macrophage migration inhibitory factor mediates peripheral nerve injury-induced hypersensitivity by curbing dopaminergic descending inhibition. *Exp Mol Med* 50:e445.
- Widerström-Noga E (2017) Neuropathic pain and spinal cord injury: phenotypes and pharmacological management. *Drugs* 77:967–984.
- Wu Z, Li L, Xie F, Du J, Zuo Y, Frost JA, Carlton SM, Walters ET, Yang Q (2017) Activation of KCNQ channels suppresses spontaneous activity in dorsal root ganglion neurons and reduces chronic pain after spinal cord injury. *J Neurotrauma* 34:1260–1270.
- Wu Z, Li L, Xie F, Xu G, Dang D, Yang Q (2020) Enhancing KCNQ channel activity improves neurobehavioral recovery after spinal cord injury. *J Pharmacol Exp Ther* 373:72–80.
- Wu Z, Yang Q, Crook RJ, O’Neil RG, Walters ET (2013) TRPV1 channels make major contributions to behavioral hypersensitivity and spontaneous activity in nociceptors after spinal cord injury. *Pain* 154:2130–2141.
- Yang Q, Wu Z, Hadden JK, Odem MA, Zuo Y, Crook RJ, Frost JA, Walters ET (2014) Persistent pain after spinal cord injury is maintained by primary afferent activity. *J Neurosci* 34:10765–10769.